AD-A040 741 CONSTRUCTION ENGINEERING RESEARCH LAB (ARMY) CHAMPAI--ETC F/G 13/13
A UNIFIED APPROACH FOR MODELING INELASTIC BEHAVIOR OF STRUCTURA--ETC(U)
MAY 77 H R JHANSALE

UNCLASSIFIED CERL-TR-M-214 NL

1 OF 1
ADA040741

END

DATE
FILMED
7-77

construction
engineering
research
laboratory

TECHNICAL REPORT M-214
May 1977
Response to Cyclic Loading

A UNIFIED APPROACH FOR MODELING INELASTIC BEHAVIOR OF STRUCTURAL METALS UNDER COMPLEX CYCLIC LOADINGS

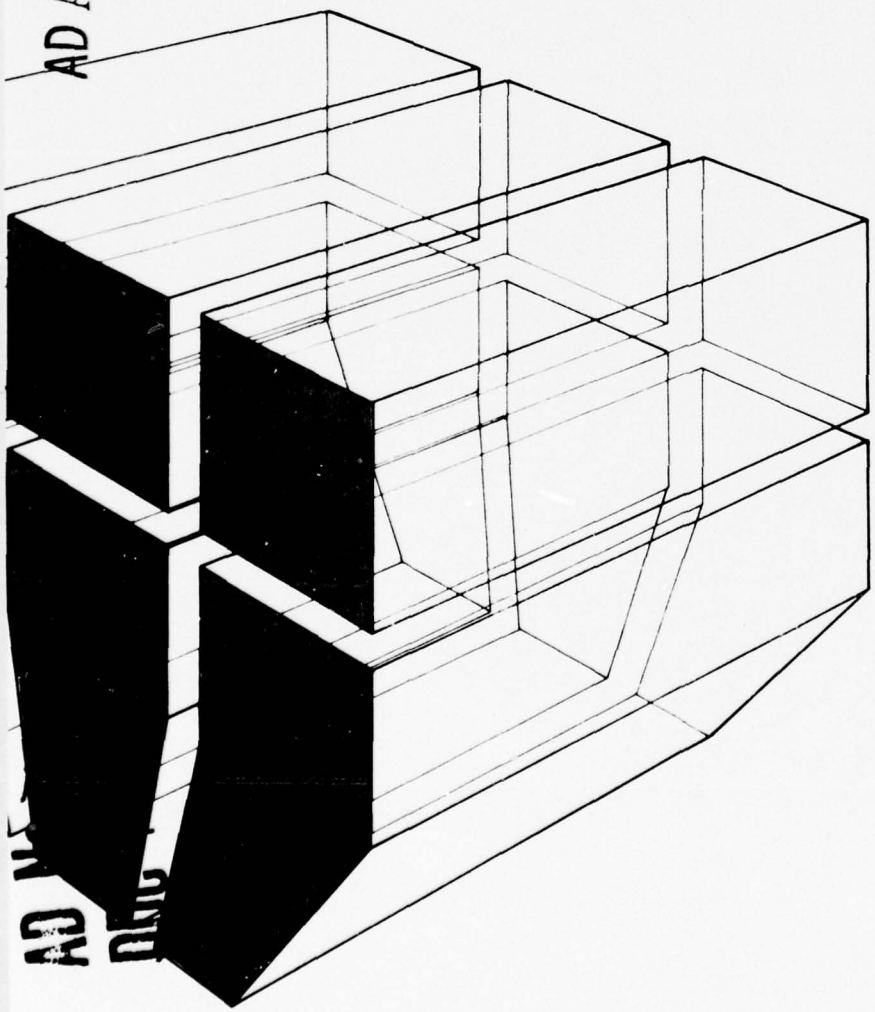

by
H. R. Jhansale

CERL

UNCLASSIFIED

SECURITY CLASSIFICATION OF THIS PAGE *(When Data Entered)*

REPORT DOCUMENTATION PAGE	READ INSTRUCTIONS BEFORE COMPLETING FORM
1. REPORT NUMBER: CERL-TR-M-214	2. GOVT ACCESSION NO. / 3. RECIPIENT'S CATALOG NUMBER
4. TITLE *(and Subtitle)*: A UNIFIED APPROACH FOR MODELING INELASTIC BEHAVIOR OF STRUCTURAL METALS UNDER COMPLEX CYCLIC LOADINGS	5. TYPE OF REPORT & PERIOD COVERED: FINAL rept. / 6. PERFORMING ORG. REPORT NUMBER
7. AUTHOR(s): H. R. Jhansale	8. CONTRACT OR GRANT NUMBER(s): T4
9. PERFORMING ORGANIZATION NAME AND ADDRESS: CONSTRUCTION ENGINEERING RESEARCH LABORATORY, P.O. Box 4005, Champaign, IL 61820	10. PROGRAM ELEMENT, PROJECT, TASK AREA & WORK UNIT NUMBERS: 4A762719AT41-T4-010
11. CONTROLLING OFFICE NAME AND ADDRESS	12. REPORT DATE: May 1977 / 13. NUMBER OF PAGES: 40
14. MONITORING AGENCY NAME & ADDRESS *(if different from Controlling Office)*: 41p.	15. SECURITY CLASS. *(of this report)*: Unclassified / 15a. DECLASSIFICATION/DOWNGRADING SCHEDULE

16. DISTRIBUTION STATEMENT *(of this Report)*

Approved for public release; distribution unlimited.

17. DISTRIBUTION STATEMENT *(of the abstract entered in Block 20, if different from Report)*

18. SUPPLEMENTARY NOTES

Copies are obtainable from National Technical Information Service
Springfield, VA 22151

19. KEY WORDS *(Continue on reverse side if necessary and identify by block number)*

inelastic stress-strain response
cyclic loading
unified modeling approach

20. ABSTRACT *(Continue on reverse side if necessary and identify by block number)*

This report develops a general procedure for modeling the inelastic stress-strain response of structural metals subjected to complex irregular cyclic loadings. The model is ideally suited for programming on a digital computer and uses "cyclic" material parameters (or properties) determined from simple constant strain amplitude cyclic tests. Four model formulations which include three degrees of simplification in the model are proposed and their appropriate applications are indicated. In its most complete formulation, the model is capable of simulating all the important observed phenomena of a wide range of structural

DD FORM 1 JAN 73 1473 EDITION OF 1 NOV 65 IS OBSOLETE 405 279 UNCLASSIFIED

SECURITY CLASSIFICATION OF THIS PAGE *(When Data Entered)*

Block 20 continued.

metals, including hotworked and coldworked steels and aircraft aluminums. These phenomena include "memory" of prior history, cyclic hardening, cyclic softening, cyclic relaxation, cyclic creep, and the observed deviation from the Masing behavior. A major contribution of this report is in the development of a unified characterization of these phenomena.

The model and the "cyclic" material parameters developed provide the necessary base for formulating a general constitutive equation in the multiaxial state of stress. Such constitutive equations are directly adoptable in the finite element codes of nonlinear structural analysis programs. The model is also useful in realistic shakedown analysis of structures and fatigue analysis of complex load histories.

FOREWORD

This investigation was conducted for the Directorate of Military Construction, Office of the Chief of Engineers (OCE) by the Structural Mechanics Branch (MSS), Materials and Science Division (MS), U. S. Army Construction Engineering Research Laboratory (CERL). The project was a part of the RDT&E Army program 6.27.19-A, Project 4A762719AT41, "Research in Military Engineering and Construction"; Task T4, "Construction Systems Technology"; Work Unit 010, "Response to Cyclic Loading." The OCE Technical Monitor was Mr. G. M. Matsumura.

The contributions to this study of Mr. S. K. Sharma and the encouragement and guidance of Dr. W. E. Fisher, Chief of MSS, are acknowledged.

Dr. G. R. Williamson is Chief of MS. COL J. E. Hays is Commander and Director of CERL, and Dr. L. R. Shaffer is Technical Director.

CONTENTS

TABLES

FIGURES

FIGURES (cont'd)

A UNIFIED APPROACH FOR MODELING INELASTIC BEHAVIOR OF STRUCTURAL METALS UNDER COMPLEX CYCLIC LOADINGS

1 INTRODUCTION

Background

The importance of analyzing seismic structures for inelastic response and low-cycle fatigue has been identified by several investigators.[1-6] These structures are designed to respond inelastically during strong-motion earthquakes both for economic reasons, and to provide effective energy dissipation and damping through plastic hysteresis. Analysis of the inelastic response of such structures is complicated by the cyclic nature of earthquake loads. Current structural analysis procedures use material constitutive equations which are only adequate for monotonic loadings. Under cyclic loading conditions, inelastic material response is complicated by two factors: (1) noncoincidence of tensile and compressive stress-strain paths resulting in hysteresis, and (2) strong dependence of stress-strain paths on prior deformation history. This concept is illustrated in Figure 1, which represents a typical stress-strain response of a material subjected to a cyclic deformation history. There is no unique relationship between stress and strain or tangent modulus and stress (or strain); these quantities are functions of their time histories. Thus, analysis of cyclic inelastic response requires a material model which can adequately simulate the observed material behavior and its prior history dependence.

[1]G. V. Berg and J. L. Stratha, *Anchorage and Alaska Earthquake* (American Iron and Steel Institute, 1964).

[2]S. A. Mahin and V. V. Bertero, "Nonlinear Seismic Response Evaluation–Charaima Building," *Proceedings ASCE, Journal of Structural Division* (June 1974), pp 1225-1242.

[3]E. P. Popov, "Low Cycle Fatigue of Connections and Details," *Proceedings ASCE-IABSE Joint International Conference on Planning and Design of Tall Buildings*, State-of-the-Art Report No. 3, Tech. Comm. No. 18, Vol II (1972), pp 741-755.

[4]C. W. Pinkham, "Procedures and Criteria for Earthquake Resistant Design–Part I," *Building Practices for Disaster Mitigation*, Building Science Series 46 (National Bureau of Standards, 1973), pp 188-208.

[5]B. Bresler, "Behavior of Structural Elements–A Review," *Building Practices for Disaster Mitigation*, Building Science Series 46 (National Bureau of Standards, 1973), pp 286-351.

[6]N. M. Newmark and E. Rosenblueth, *Fundamentals of Earthquake Engineering* (Prentice Hall, Inc., 1971).

Objective

The objective of this report is to develop a unified approach for modeling the uniaxial inelastic behavior of structural metals appropriate for irregular cyclic loading conditions. Development of appropriate material parameters required for such a model is also included in this objective. The model will be digital-computer-oriented and suitable for numerical procedures in structural mechanics and failure analysis.

Approach

It is convenient to distinguish two features of cyclic inelastic behavior of structural metals for the purpose of modeling. These features are termed the "memory" phenomenon (Chapter 2) and "plastic hysteresis" phenomena (Chapter 3). Excellent models of simulating memory are available[7-11] and the one best suited for the present purpose will be adopted. By extending recent studies[12, 13] on the plastic hysteresis phenomena, a unified approach for their quantitative description will be developed and combined with the memory model to obtain a complete characterization of material behavior. Chapter 4 discusses the material properties required by the model and the tests for determining those properties. Chapter 5 discusses the synthesis of memory model and plastic hysteresis phenomena, some appropriate simplifcations in the model, and typical simulations for two materials. Chapter 6 outlines three

[7]W. D. Iwan, "On a Class of Models for the Yielding Behavior of Continuous and Composite Systems," *Transactions of ASME, Journal of Applied Mechanics* (September 1967).

[8]P. C. Jennings, "Earthquake Response of a Yielding Structure," *Proceedings ASCE, Journal of Engineering Mechanics Division*, Paper No. 4435, EM 4 (August 1965), pp 41-68.

[9]J. F. Martin, T. H. Topper, and G. M. Sinclair, "Computer Based Simulation of Cyclic Stress-Strain Behavior With Applications to Fatigue," *Materials, Research and Standards, MTRSA*, Vol 11, No. 2, (February 1971), pp 23-29.

[10]H. R. Jhansale and T. H. Topper, "An Engineering Analysis of the Inelastic Stress Response of a Structural Metal Under Variable Cyclic Strains," *Cyclic Stress-Strain Behavior–Analysis, Experimentation and Failure Prediction*, ASTM STP 519 (American Society for Testing and Materials [ASTM], 1973).

[11]R. M. Wetzel, *A Method of Fatigue Damage Analysis*, Technical Report No. SR 71-107 (Ford Motor Company, August 1971).

[12]H. R. Jhansale, "A New Parameter for the Hysteretic Stress-Strain Behavior of Metals," *Transactions of ASME, Journal of Engineering Materials and Technology*, Vol 97, Series H, No. 1 (January 1975), pp 33-38.

[13]H. R. Jhansale, "A Friction Stress Method for the Cyclic Inelastic Behavior of Metals," *Transactions of the 3rd International Conference on Structural Mechanics in Reactor Technology*, Vol 5, L5/4 (September 1975).

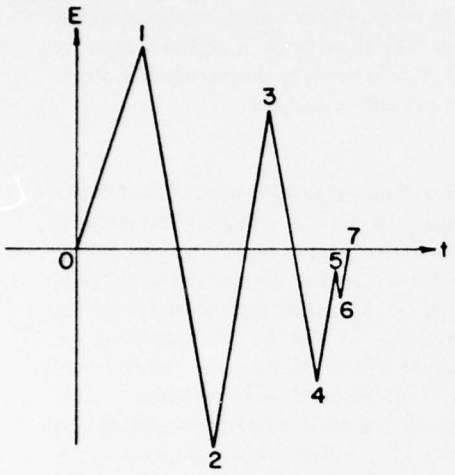

STRAIN-TIME INPUT

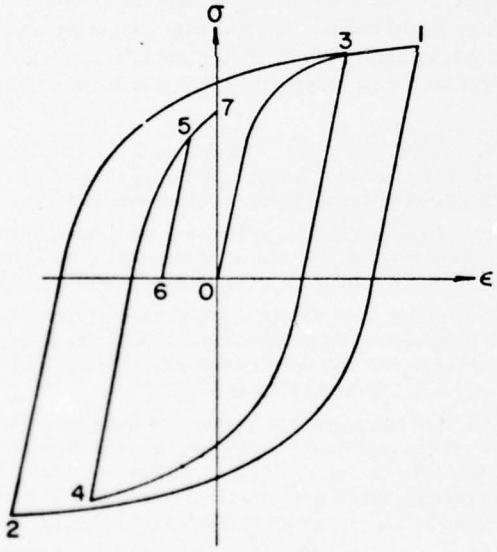

STRESS-STRAIN RESPONSE

Figure 1. Typical cyclic inelastic material response.

applications of structural mechanics and failure analysis for this research.

Mode of Technology Transfer

The results of this study will impact TM 5-809-10, *Seismic Design for Buildings*.[14]

2 MEMORY PHENOMENON

The memory phenomenon can be best described by two simple examples, as shown in Figure 2. If the material is loaded through OA, as shown in Figure 2a, then unloaded through AB, and finally loaded in the tensile direction, it apparently "remembers" the previous point, A, of unloading and follows the path AC, which would be the path if the material were not unloaded at A. Thus, there is a discontinuity in the stress-strain response during the loading BC at A. Similarly, in the second example (Figure 2b), the final stress-strain path, DE, is composed of two discontinuities, C and A. Segments CA and AE are continuations of BC and OA, respectively. The memory phenomenon accounts for the internal stress distribution caused by the previous loading history.

Model for Memory

A rheological model consisting of linear elastic springs and solid friction sliders such as the one shown in Figure 3 is commonly used to simulate the memory phenomenon. By choosing an appropriate number of spring-slider elements, stiffnesses for the springs, and friction stresses for the sliders, the nonlinear stress-strain characteristic of the material can be matched as accurately as desired with a piecewise linear approximation. The model also exhibits the so-called Baushinger effect, which is characterized by a decrease in the yield stress level in the reverse direction after plastic deformation. Based on this rheological model, several formulations for simulating the memory phenomenon have been proposed.[15, 16] The approach which uses a

---

[14] *Seismic Design for Buildings*, TM5-809-10 (Department of the Army, 1973). This TM is also published by the Navy and Air Force as NAVFAC P-355 and Chapter 13 of AFM88-3, respectively.

[15] J. F. Martin, T. H. Topper, and G. M. Sinclair, "Computer Based Simulation of Cyclic Stress-Strain Behavior with Applications to Fatigue," *Materials, Research and Standards, MTRSA*, Vol 11, No. 2, (February 1971), pp 23-29.

[16] R. M. Wetzel, *A Method of Fatigue Damage Analysis*, Technical Report No. SR 71-107 (Ford Motor Company, August 1971).

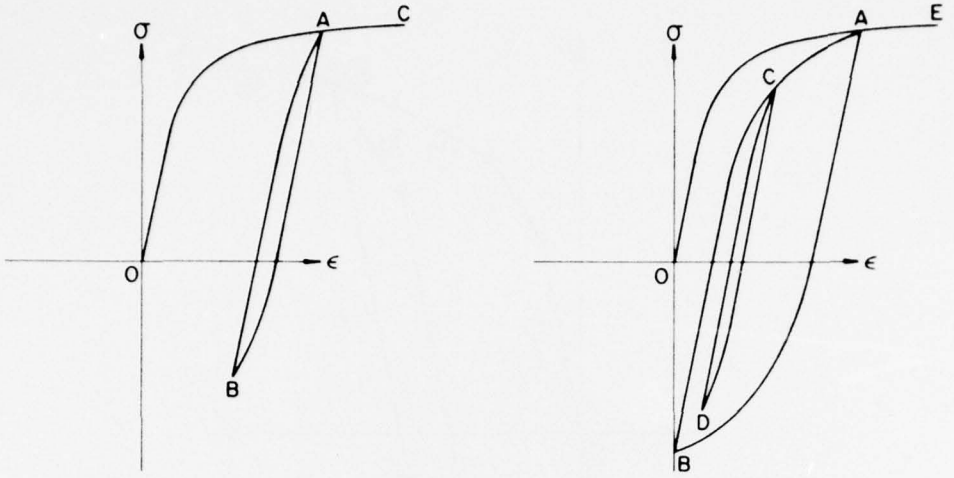

(a) (b)

Figure 2. Two examples of memory phenomenon.

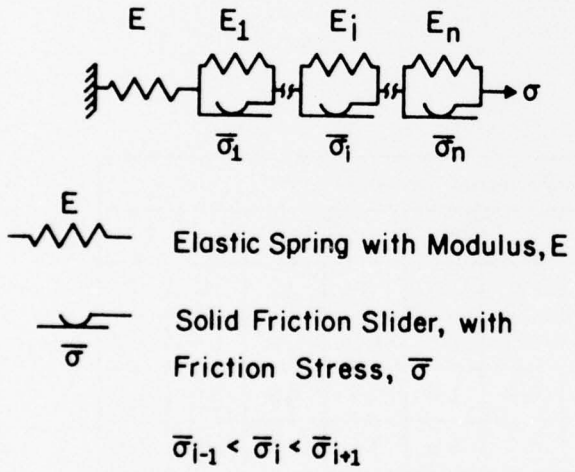

Figure 3. Rheological model.

set of simple rules is ideally suited for digital computation and will be adopted.[17] These rules will be illustrated with the aid of the following example.

Methods of Memory Rules

The initial stress-strain curves for tension and compression are assumed to be identical. The stress-strain curves can be approximated by a set of piecewise linear segments whose lengths, slopes, and number are suitably chosen. Figure 4 illustrates a five-segment curve. The memory rules are as follows:

1. The availability of a segment during the current loading path which is either tensile or compressive depends on the prior loading history and is denoted by an "availability coefficient" in that direction.

2. The absolute sum of the availability coefficients in the tensile and the compressive directions for *each* segment is always equal to *two*. The initial availability coefficient in tension or in compression for *each* segment is *one*.

3. During a specific loading, the stress-strain path is defined by segments, starting with the first, and proceeding in consecutive order to the extent that the segments are available in the direction of loading until the desired stress or strain limit is reached.

4. The availability of a segment in a given direction (tension or compression) decreases to the extent it is used in that direction, but increases by that amount in the opposite direction in conformity with rule 2.

In brief, the procedure amounts to a simple bookkeeping operation of the availability coefficients as illustrated in Figure 4. When the tensile loading sequence

[17] R. M. Wetzel.

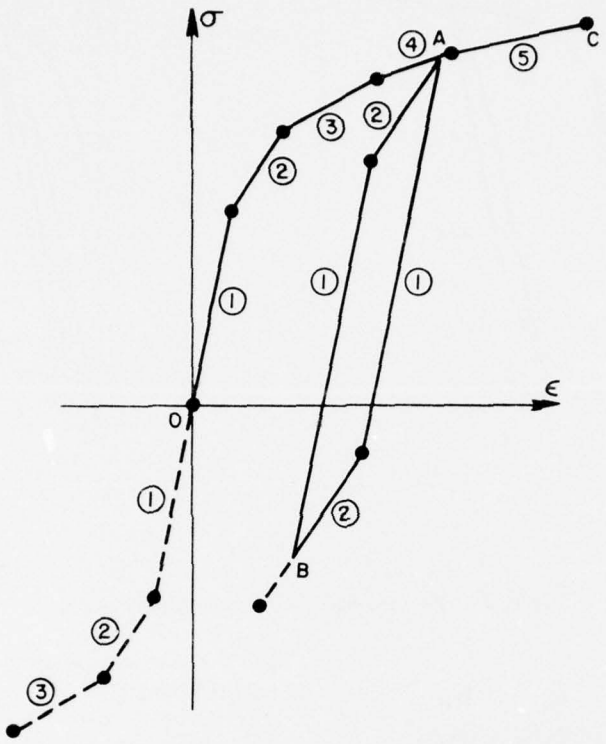

Loading Path			Availability Coefficient of Elements									
			①		②		③		④		⑤	
			T	C	T	C	T	C	T	C	T	C
OA	T	S	1.0	1.0	1.0	1.0	1.0	1.0	1.0	1.0	1.0	1.0
		E	0.0	2.0	0.0	2.0	0.0	2.0	0.2	1.8	1.0	1.0
AB	C	S	0.0	2.0	0.0	2.0	0.0	2.0	0.2	1.8	1.0	1.0
		E	2.0	0.0	1.3	0.7	0.0	2.0	0.2	1.8	1.0	1.0
BC	T	S	2.0	0.0	1.3	0.7	0.0	2.0	0.2	1.8	1.0	1.0
		E	0.0	2.0	0.0	2.0	0.0	2.0	0.0	2.0	0.0	2.0

(S - Start, E - End, T - Tension. C - Compression, Unused Elements Underlined)

Figure 4. Example for illustrating memory rules. Reprinted with permission of Ford Motor Company from R. M. Wetzel, *A Method of Fatigue Damage Analysis*, Technical Report No. SR71-107 (August 1971).

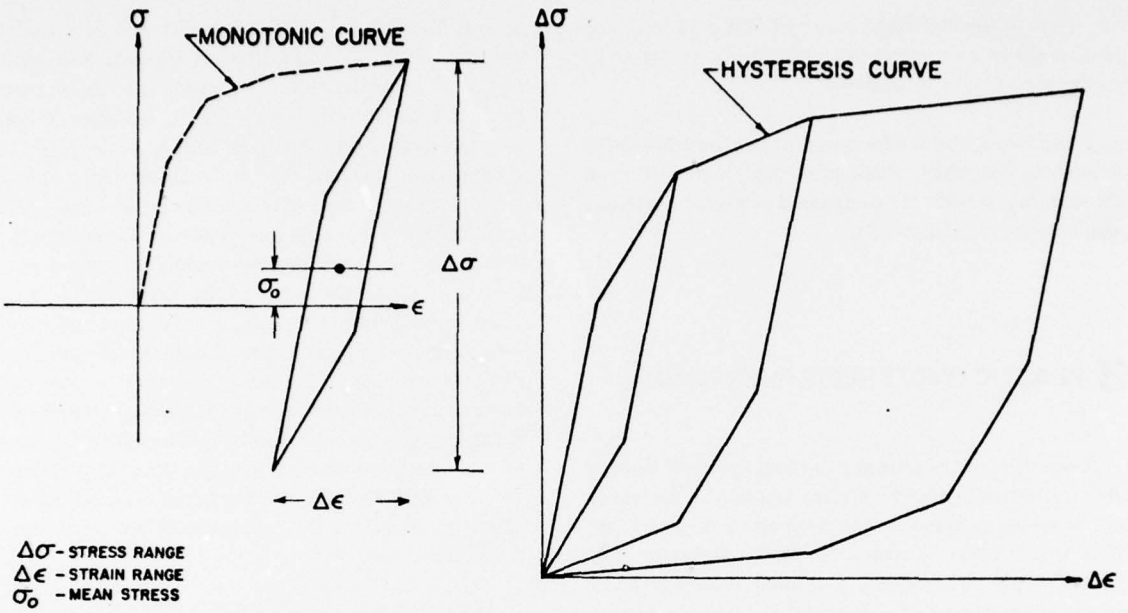

(a) Stable closed loop behavior under mean stress.

(b) Identically shaped hysteresis branches (yield range is constant).

Figure 5. Masing and stable responses of memory model.

OA begins, one unit of each segment is available in tension and compression. Hence, the stress-strain path OA consists of one-unit lengths of elements 1 to 3 and 0.8 unit of 4; at this stage, point A is reached. The availability coefficients of these segments in tension are reduced by the amounts of these element lengths, but at the same time, their availability coefficients in compression are correspondingly increased by the same amount. The availability coefficients of segment 5 are unaltered, since that segment was not used. The next loading sequence, AB, which is compressive, uses the two available units of segment 1 and 1.3 units of segment 2; at this stage, the desired limit B is reached. The next sequence, BC, which is tensile, uses the two units of 1, 1.3 units of 2, none of 3, 0.2 units of 4, and one unit of 5; at this stage, point C is reached. Thus, the memory phenomenon has been successfully simulated by recognizing the unloading point A and producing stress-strain path AC, which is the continuation of OA.

Memory Model Vs. Real Materials

Under constant stress or strain range cycling, the rheological model (or the method of rules) produces fully closed hysteresis stress-strain loops, even in the presence of a mean stress or mean strain as illustrated in Figure 5. Although real materials eventually approach this stable (or saturation) state in the limit, they usually exhibit a prior transient behavior (to be fully described in Chapter 3) during which hysteresis paths gradually change from cycle to cycle. This transient behavior is particularly pronounced in the presence of a mean stress.

The hysteresis curves produced by the rheological model (or the method of rules) are geometrically similar to the monotonic stress-strain curve but magnified by a scale factor of two. This occurs because in order to reverse the sliding direction for a slider, it is necessary to apply a stress range which is twice that of the slider's friction stress. This property, originally postulated by Masing, is often referred to as Masing postulation (or Masing behavior).[18] It also implies that the linear elastic portion or yield range (which is twice the yield strength) is independent of the hysteresis loop size (or strain or stress amplitude). For example, if various sized hysteresis loops produced by the model are superimposed on their lower tips, the upper hysteresis paths are coincident, as shown in Figure 5b. Many real mater-

[18] G. Masing, "Eigenspannungen und Verfestigung bein Messing," *Proceedings of the 2nd International Congress of Applied Mechanics, Zurich 1926* (1926), pp 332-335.

ials, even in the stabilized state, exhibit a variation of yield range as a function of loop size. These materials are denoted as non-Masing type.

These two features (the transient and the non-Masing characteristics which distinguish real materials from the memory model) are designated as plastic hysteresis phenomena (see Chapter 3).

3 PLASTIC HYSTERESIS PHENOMENA

A recent study of several structural metals[19] showed that the various cycle-dependent transient phenomena and non-Masing behavior can be characterized in terms of a single history-dependent stress parameter. The present study has yielded additional insight into the quantitative aspects of this parameter and its history dependence. This chapter describes these findings and provides a suitable model for characterizing the plastic hysteresis phenomena.

Observed Transient Phenomena

The transient phenomena are classified into four types (Figure 6) and are designated as cyclic hardening, cyclic softening, cyclic relaxation, and cyclic creep. As illustrated in Figures 6a and 6b, cyclic hardening or softening is denoted by a cycle-dependent increase or decrease in stress range under constant strain range cycling. Similarly, under constant stress range cycling, these two phenomena manifest as changes in the strain range. Cyclic relaxation is denoted by a cyclic-dependent decrease in the absolute mean stress under constant strain range cycling, whereas cyclic creep is denoted by a cycle-dependent increase in the absolute mean strain under constant stress range cycling. Figures 6c and 6d schematically illustrate cyclic relaxation of a tensile mean stress and cyclic creep in tension, respectively. A material can simultaneously exhibit cyclic hardening or softening and cyclic creep or relaxation.

Extensive experimental observations of the transient behavior of many different structural metals made by several investigators during the past two decades[20-23] can be generally summarized as follows. Soft metals (e.g., hotworked) cyclically harden and hard metals (e.g., coldworked) cyclically soften. However, initially soft but strain-aged materials, such as hotworked common structural steels, exhibit cyclic softening at lower strain amplitudes and cyclic hardening at higher strain amplitudes. This apparent anomalous softening is believed to be caused by the gradual unpinning of dislocations which were locked by interstitial impurity atoms during the strain-aging process. One feature of a softening phenomenon that should be of concern in deformation analysis is the fact that what appears to be a linear elastic response during the initial period of cyclic loading will eventually develop into inelastic hysteresis response with continued cycling as illustrated in Figure 7. Thus, analysis based on the initial stress-strain characteristic could result in nonconservative estimates of deformation response.

The initial cyclic hardening or softening phenomenon is transient, and a state of saturation is approached at a continuously decreasing rate with cycles. This stable or saturated state is usually maintained with continued cycling at constant amplitude until fatigue cracks initiate. However, each time the stress or strain amplitude (or limit) is changed from one level to another, a transient behavior ensues even though the material has been initially saturated. This transient behavior is comprised of both hardening or softening and relaxation or creep. Specific data illustrating these various aspects of observed transient behavior are discussed in the following sections dealing with the quantitative characterization of these phenomena.

Analysis of Hysteresis Loops

A hysteresis loop has two branches: the upper branch corresponds to the tensile loading direction, and the lower branch corresponds to the compressive direction. During the transient conditions, a hysteresis loop is not closed, and the hysteresis branches are not identical (see Figure 6); however, in the saturated state, the hys-

[19] H. R. Jhansale, "A New Parameter for the Hysteretic Stress-Strain Behavior of Metals," *Transactions of ASME, Journal of Engineering Materials and Technology*, Vol 97, Series H, No. 1 (January 1975), pp 33-38.

[20] L. F. Coffin, Jr. and J. F. Tavernelli, "The Cyclic Straining and Fatigue of Metals," *Transactions of the Metallurgical Society, AIME*, Vol 215 (October 1959), pp 794-806.

[21] F. R. Tuler and J. Morrow, *Cycle Dependent Stress-Strain Behavior of Metals*, T&AM Report No. 293 (University of Illinois, March 1963).

[22] R. W. Landgraf, *Cyclic Deformation and Fatigue of Hardened Steels*, T&AM Report 320 (University of Illinois, 1968).

[23] S. Keshaven, *Some Studies on the Deformation and Fracture of Normalized Mild Steel Under Cyclic Conditions*, Ph.D. Dissertation (University of Waterloo, December 1966).

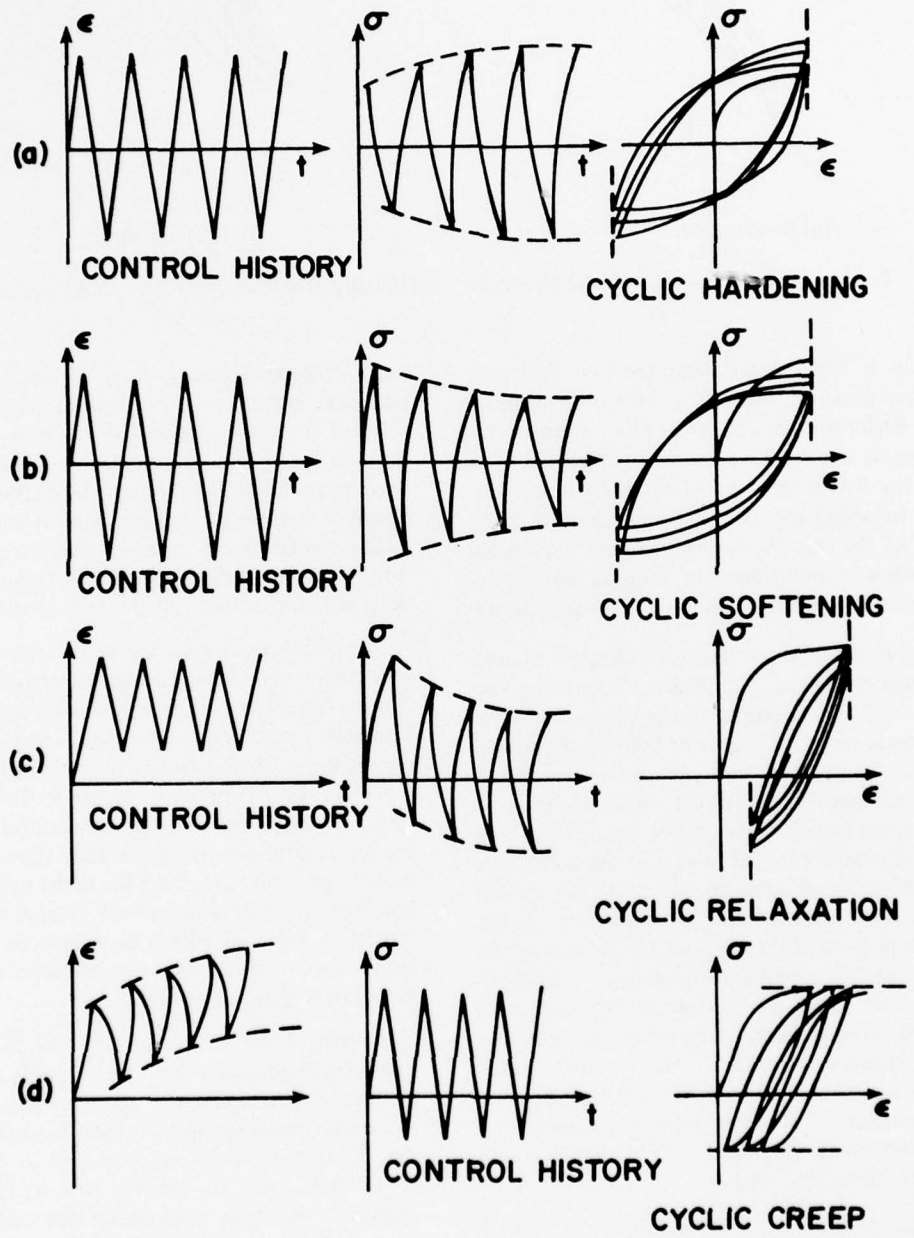

Figure 6. Classification of cyclic transient phenomena.

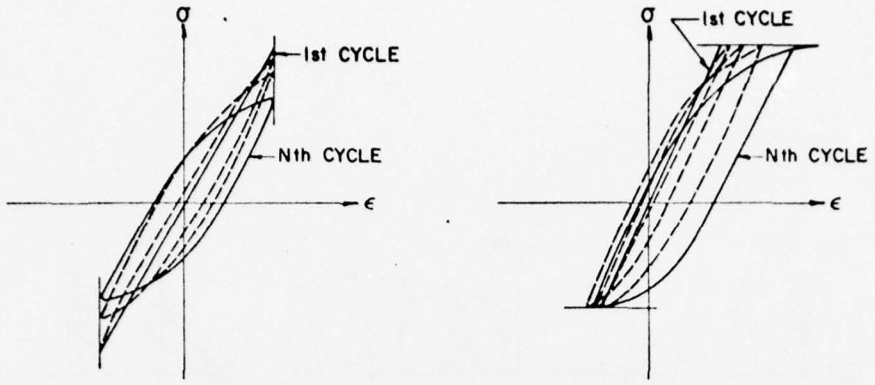

(a) Stress control. (b) Stress control.

Figure 7. Gradual development of inelastic hysteresis from initially elastic behavior in cyclically softening materials.

teresis loop is fully closed, and the two hysteresis branches are identical, one being the mirror image of the other. Each branch is designated as a "reversal," and cyclic progress is denoted in terms of the number of reversals. The first reversal is the hysteresis branch immediately following the first monotonic loading at the beginning of the test. As a rule, the first monotonic loading path is treated separately from the other cyclic loading paths, and no reversal number is assigned to it.

A recent study of several structural metals[24] showed that transient changes in the hysteresis branches are essentially caused by changes in the lengths of the initial "linear" elastic parts. The slope of the "linear" elastic portions and the shape of the nonlinear portions remain virtually unchanged (see Figure 8, in which the first three hysteresis branches of a typical cyclic hardening situation are compared). The change in the elastic part is designated as "yield range increment" (YRI), since it denotes a change in the yield range of the material. The yield range is twice the yield strength because of the scale factor of two between the monotonic and hysteretic stress-strain paths (see Chapter 2). Physically, this change in the yield strength (or range) is caused by substructural changes associated with reversed plastic straining in a cyclic situation. Thus, transient phenomena can be described in terms of a simple parameter YRI or "yield strength increment" (YSI), which is one-half of YRI. The elastic modulus can be assumed to remain unchanged during cyclic loading. The invariant nonlinear portion of the hysteresis branch that is unaffected by the cyclic plastic straining represents an intrinsic material property. Denoting such an intrinsic stress-strain curve as "skeleton stress-strain curve," the invariant nonlinear hysteresis branch will be geometrically similar to the skeleton stress-strain curve, but magnified by a scale factor of two. Chapter 4 discusses determination of the skeleton stress-strain curve.

A reversal to reversal increase or decrease in YRI denotes hardening or softening, respectively, whereas a relative difference in YRI between the upper and lower hysteresis branches describes cyclic creep or relaxation, depending on the controlled limits (stress or strain), as schematically illustrated in Figure 9. The relative difference in YRIs between two consecutive reversals decreases as saturation is approached. Therefore, in a saturated hysteresis loop, the YRIs in the upper and lower branches are equal in magnitude. In most materials, the saturation value of YRI is dependent on the stress or strain amplitude. These materials were designated as non-Masing type in Chapter 2.

As part of the present investigation, all the observations discussed above have been verified for a large number of structural metals ranging widely in strengths and cyclic characteristics. Analysis of available data on the elevated temperature combined cyclic and hold period (static relaxation/creep) tests on two high-temperature alloy steels also indicate that both cyclic transient and static creep/relaxation behavior can be described in terms of changes in YRI. Table 1 summarizes the materials studied and observations about them. Only typical results are discussed in the following section.

[24] H. R. Jhansale, "A New Parameter for the Hysteretic Stress-Strain Behavior of Metals, *Transactions of ASME, Journal of Engineering Materials and Technology*, Vol 97, Series H, No. 1 (January 1975), pp 33-38.

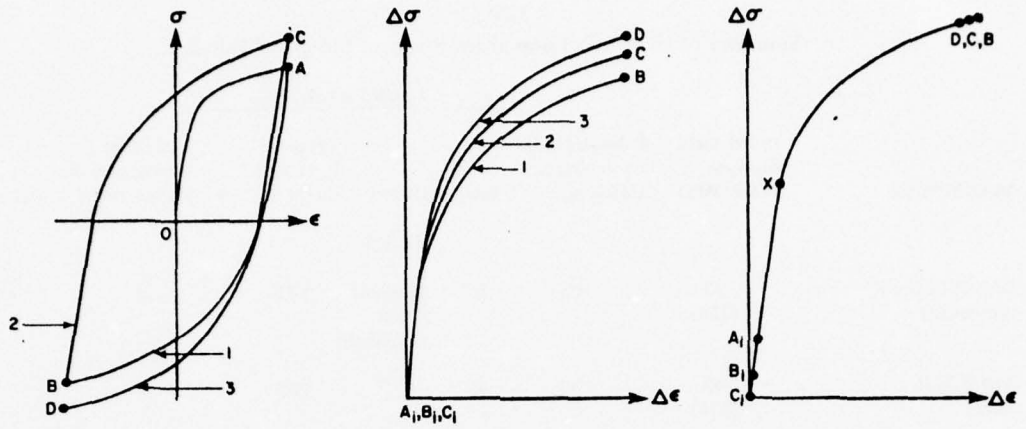

(a) Three hysteresis reversals of cyclic hardening.

(b) Three reversals are superimposed on their initial points A_i, B_i, and C_i, respectively.

(c) Reversals 1 and 2 are translated along linear elastic slope to match nonlinear portions. Curve A_iXDCB is a doubled skeleton stress-strain curve; linear parts A_i, B_i, and A_iC_i are YRIs of reversals 2 and 3, respectively. YRI of reversal 1 is zero.

Figure 8. Comparison of first three hysteresis branches of a typical hardening situation.

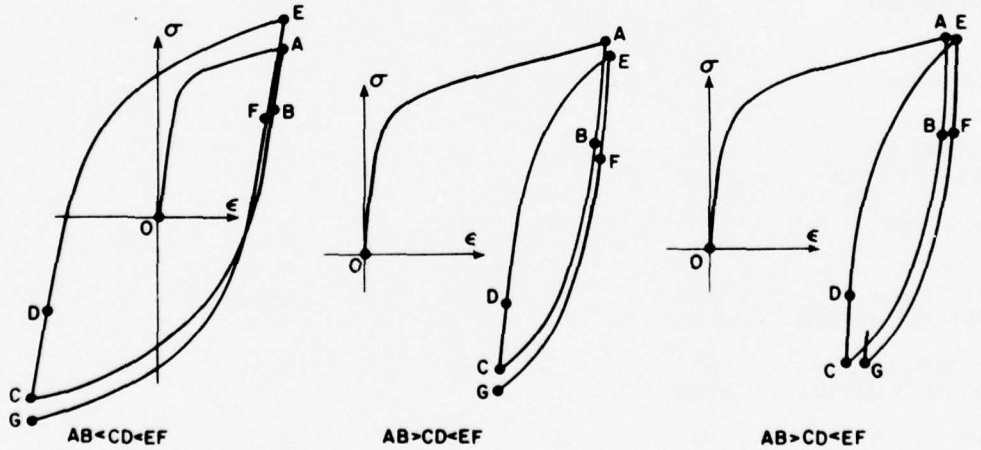

(a) Cyclic hardening.

(b) Cyclic relaxation.

(c) Cyclic creep.

Figure 9. Reversal to reversal variation in YRI during transient behavior. AB, CD, and EF are YRIs corresponding to reversals AC, CE, and EG. Portions BC, DE, and FG are identical in shape and are described by doubled skeleton stress-strain curves.

Table 1
Summary of Hysteresis Loop Shape Study of Structural Metals

No.	Material Name	Initial Yield Strength in ksi (MPa)	Exhibits Cyclic Hardening or Softening	Conditions of Test: Temp.	Conditions of Test: History	Types of Hysteresis Loops Studied	Is Material Masing or Non-Masing Type?	Data Source
				STEELS				
1	SAE 1018 Steel normalized	33 (228)	H/S	RT	Constant Strain Amplitude	T&St	N	a, b
2	ASTM A-36 steel	40 (276)	H/S	RT	"	T&St	N	c
3	SAE 1045 steel normalized	45 (311)	H/S	RT	"	T&St	N	d
4	ASTM A-440 steel (Man-Ten)	46 (317)	H/S	RT	"	St	N	e
5	Hadfied steel	60 (414)	H	RT	"	St	N	f
6	EN25 steel Q&T (450°C) British	90 (621)	S	RT	"	T	N	g
7	SAE 1045 steel Q&T (1200°F [649°C])	92 (635)	S	RT	"	T&T	N	h
8	SAE 4340 steel	100 (690)	S	RT	"	St	N	i
9	Cast 8630 steel	103 (711)	S	RT	"	T&St	N	j
10	RQC-100 steel	130 (897)	S	RT	"	St	N	k
11	SAE 1045 steel Q&T 720°F [382°C]	185 (1277)	S	RT	"	T&St	N	h
12	Mar 200 steel	215 (1484)	S	RT	"	St	N	h
13	SAE 1045 steel (Q&T (500°F [260°C])	245 (1691)	S	RT	"	T&St	N	h
14	SAE 1045 steel Q&T (360°F [182°C])	260 (1794)	S	RT	"	T&St	M	h
15	SAE 1045 steel as quenched	265 (1829)	St	RT	"	St	M	d
16	Ausformed H-11 steel	295T (2036) 365C (2519)	St	RT	"	St	M	l

Table 1 (Continued)
Summary of Hysteresis Loop Shape Study of Structural Metals

No.	Material Name	Initial Yield Strength in ksi (MPa)	Exhibits Cyclic Hardening or Softening	Conditions of Test: Temp.	Conditions of Test: History	Types of Hysteresis Loops Studied	Is Material Masing or Non-Masing Type?	Data Source
17	AISI 304 Stainless Steel	10 (69)	H	1100F	constant strain cycling & static creep and relaxation during holds.	T&St	N	m
18	2 1/4 CR-1 Mo steel	26 (179)	H	950F	"	T&St	N	n
				OTHER METALS				
19	OFHC copper annealed	03 (16.7)	H	RT	constant strain cycling	St	N	b
20	2024-T4 aluminum	55 (380)	H	RT	"	T&St	M	d, o
21	7075-T6 aluminum	68 (469)	H	RT	"	T&St	M	d

Legend: H–Hardening; S–Softening; T–Transient; St–Stable; M–Masing type, N–Non-Masing type; *RT–Room Temperature.*

a S. Keshaven, *Some Studies on the Deformation and Fracture of Normalized Mild Steel Under Cyclic Conditions,* Ph.D. Dissertation (University of Waterloo, December 1966).

b H. R. Jhansale, *Inelastic Deformation and Fatigue Response of Spectrum Loaded Strain Controlled Axial and Flexural Members,* Ph.D. Dissertation (University of Waterloo, March 1971).

c J. F. Martin, *Cyclic Mechanical Tests and an Appropriate Analytical Stress-Strain Model for A-36 Steel,* Technical Report M-36/AD780802 (U. S. Army Construction Engineering Research Laboratory, May 1974).

d H. R. Jhansale, unpublished experimental studies, H. F. Moore Fracture Lab (University of Illinois, 1973-74).

e P. C. Rosenberger, *Fatigue Behavior of Smooth and Notched Specimens of Man-Ten Steel,* M. S. Thesis (T&AM Department, University of Illinois, 1968).

f R. C. Rice and R. I. Stephens, *Overload Effects on Sub-Critical Crack Growth in Austenitic Manganese Steel,* ASTM STP 536 (1973).

g P. W. J. Oldroyd, D. J. Burns, and P. P. Benham, "Strain Hardening and Softening of Metals Produced by Cycles of Plastic Deformation," *Proc. Institution of Mechanical Engineers,* Vol 150 (1965-66).

h R. W. Landgraf, unpublished experimental data, Graduate Research Program (T&AM Department, University of Illinois, 1966-68).

i R. W. Smith, M. H. Hirschberg, and S. S. Manson, *Fatigue Behavior of Materials in Low and Intermediate Life Range,* NASA Technical Note D-1574 (National Aeronautics and Space Administration, April 1963).

j D. F. Dittmer and M. R. Mitchell, *Material Characterization of Cast 8630 Steel: Monotonic and Cyclic Stress-Strain Behavior and Strain-life Response,* FCP Report No. 13 (College of Engineering, University of Illinois, October 1974).

k L. E. Tucker, unpublished material information record (Materials Engineering Department, Deere & Co., 1972).

l J. E. Methany, Jr., unpublished experimental data, Graduate Research Program (T&AM Department, University of Illinois, 1967-68).

m R. W. Swindeman, unpublished experimental data (Metals and Ceramics Division, Oak Ridge National Laboratory, 1975).

n C. E. Jaske, B. N. Leis, and C. E. Pugh, "Monotonic and Cyclic Stress-Strain Response of Annealed 2 1/4 cr - 1 Mo Steel," *Structural Materials for Service at Elevated Temperatures in Nuclear Power Generation,* MPC-1 (American Society of Mechanical Engineers, 1975).

o JoDean Morrow, unpublished data from graduate course notes (T&AM Department, University of Illinois, Spring 1973).

Observed Typical Yield Range Increment (YRI) Behavior

Most materials can be classified into three general groups, depending on the type of initial transient behavior they exhibit. These are (1) materials which exhibit initial cyclic hardening, (2) materials which exhibit initial cyclic softening, and (3) materials which exhibit initial cyclic softening or hardening depending on the strain amplitude. The observed YRI behavior will be discussed in terms of these three groups.

First Reversal and Saturation YRIs

The values of YRI corresponding to the first reversal and cyclic saturation state are plotted as functions of strain amplitude for three typical materials (each representing a different group) in Figures 10, 11, and 12. For each material, the YRI corresponding to the state which has the minimum linear elastic portion in the hysteresis curve is assigned a zero value. The YRIs of all other hysteresis branches are measured with respect to this datum and therefore are always positive.

In the case of 2024-T4 aluminum, which is initially soft and exhibits cyclic hardening, the saturation YRI corresponding to the hardened state is larger than the first reversal value shown in Figure 10. The first reversal value is approximately zero, and both the initial and saturation values of YRI are essentially independent of strain amplitude. Consequently, the hysteresis branches of various sized saturation loops are identical in shape, as shown in Figure 13, in which fully reversed hysteresis loops are superimposed on their lower tips. As shown in Table 1, 2024-T4 is one of the few materials observed that exhibit Masing behavior. A comparison of the saturation YRIs obtained under constant amplitude cycling and mixed prior cyclic history shown in Figure 10 indicates that the saturation YRI is relatively insensitive to prior cyclic history.

In the case of SAE 1045 quenched and tempered steel, which is initially hard and exhibits cyclic softening, both the first reversal and saturation YRIs are dependent on strain amplitude, as illustrated in Figure 11. Consistent with this softening phenomenon, the saturation YRI is less than the first reversal YRI. Cold-worked structural steels are generally expected to exhibit these characteristics.

In the case of common structural steels (initially hotworked) which exhibit initial cyclic softening or hardening depending on strain amplitude, the first reversal and saturation YRIs vary with strain, as typically shown for A-36 steel in Figure 12. The initial high value of YRI corresponding to small strains is due to the strain-aged condition of the material. The sudden drop in the initial YRI on the application of a small monotonic strain is due to the unpinning of dislocations which were locked by interstitial impurity atoms during strain aging. This phenomenon is also manifested in the "upper and lower yield point" behavior of steels. At smaller strain levels, where the first reversal YRI is larger than the saturation YRI, the material exhibits cyclic softening and higher strain levels; where the saturation YRI is larger than the first reversal, YRIs are associated with cyclic hardening. The non-Masing behavior, signified by the dependence of saturation YRI on strain amplitude, is well illustrated in Figure 14, in which saturated, fully reversed hysteresis loops of various sizes are compared by superimposing them on their lower tips. The upper branches do not match; however, by sliding the individual loops along the elastic slope, the upper branches can be matched extremely well, as shown in Figure 15. The difference in the linear elastic portions between different sized loops is due to the dependence of YRI on strain amplitude. As shown in Figure 12, the saturation YRI appears to be somewhat sensitive to prior cyclic history at smaller strains and not at higher strains. Past microstructural studies[25] have shown that low- and high-strain levels are generally associated with widely different substructures; it is rather difficult to revert from the one corresponding to the higher strain level to the one corresponding to lower levels, when higher strain levels are preceded by lower one, but not vice versa.

Variation of YRI During Cyclic Hardening/Softening

To measure the variation of YRI during cyclic hardening/softening, it is necessary to analyze the transient hysteresis loops under constant amplitude cycling. Such transient hysteresis loop data were available for three materials representing the three general groups mentioned previously—SAE 1045 normalized steel, 2024-T4 aluminum, and SAE 1045 quenched and tempered (720°F [378°C]) steel. It was observed that in all three materials, the rate of YRI change per reversal at a given strain amplitude decreased as saturation was approached and the number of reversals increased. Therefore, the following general expression for the rate of change of yield strength was assumed for analyzing the data:

[25] C. E. Feltner and C. Laird, "Cyclic Stress-Strain Response of FCC Metals and Alloys, I-Phenomenological Experiments, II-Dislocation Structures and Mechanisms," *Acta Metallurgica*, Vol 15 (1967).

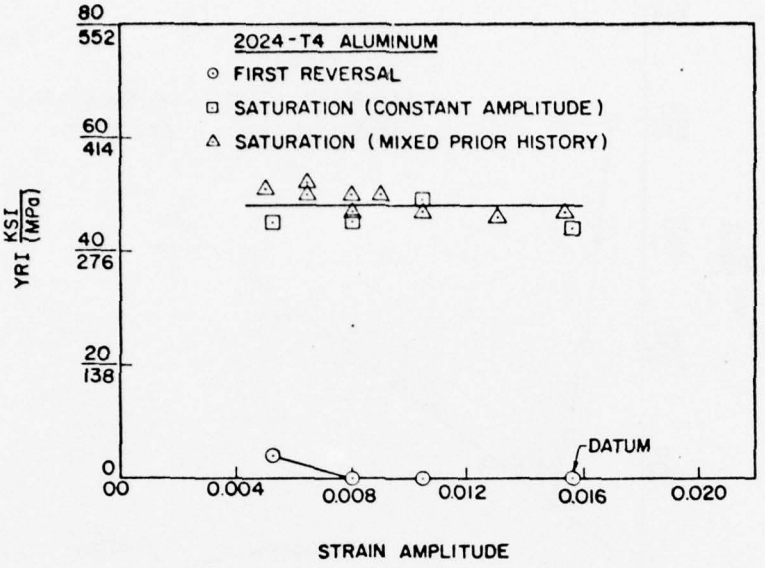

Figure 10. First reversal and saturation YRIs of 2024-T4 aluminum expressed as functions of strain amplitude.

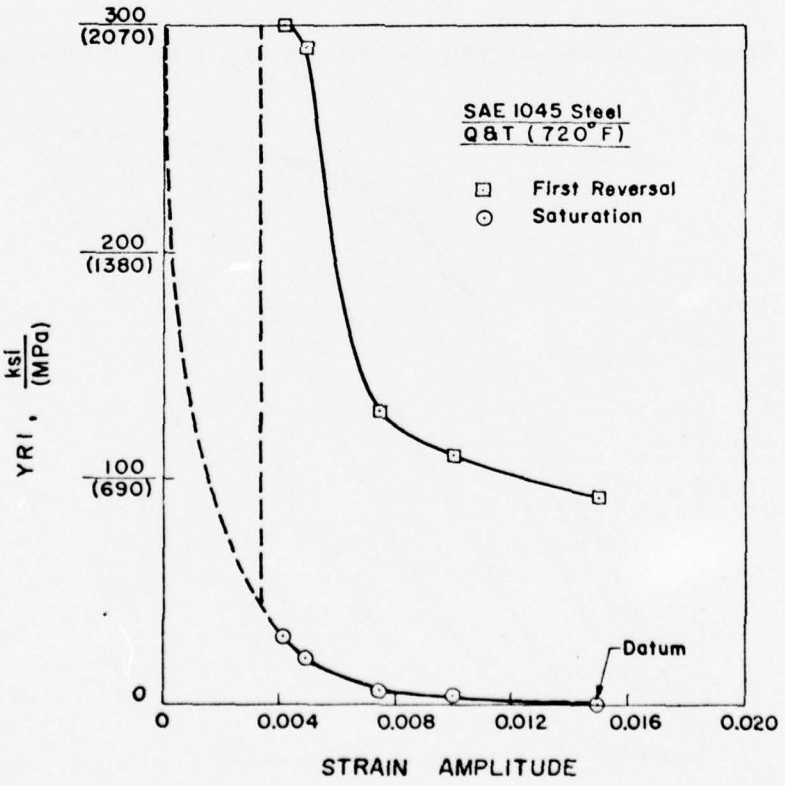

Figure 11. First reversal and saturation YRIs of SAE 1045 quenched and tempered (720°F [378°C]) steel expressed as functions of strain and amplitude.

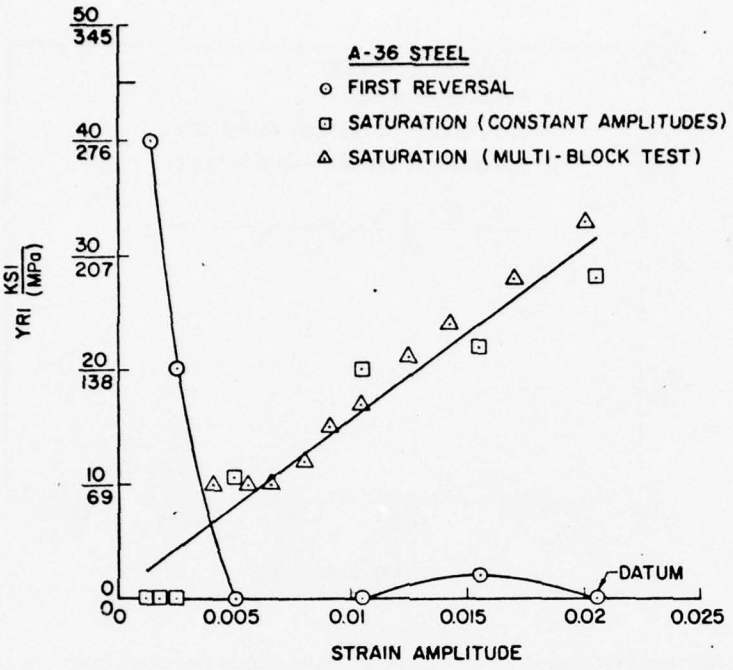

Figure 12. First reversal and saturation YRIs of A-36 steel expressed as functions of strain amplitude.

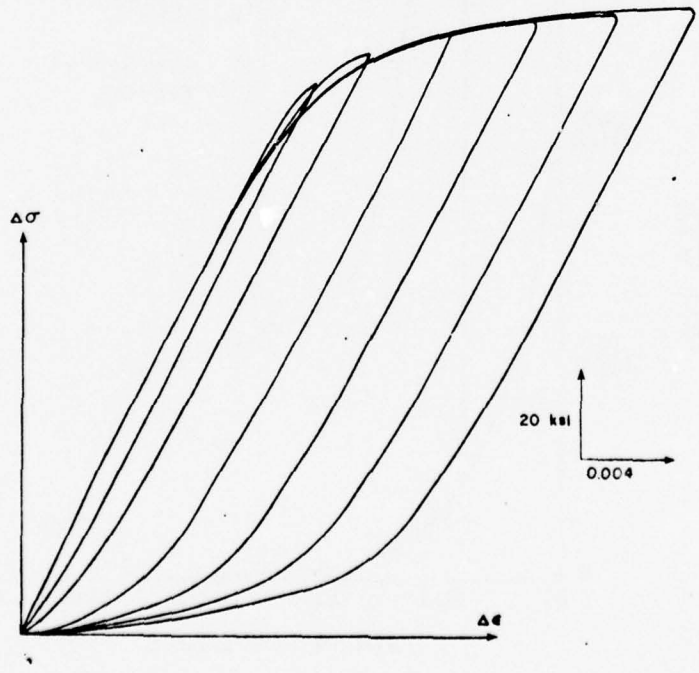

Figure 13. Fully reversed saturation hysteresis loops of 2024-T4 aluminum superimposed on their lower tips.

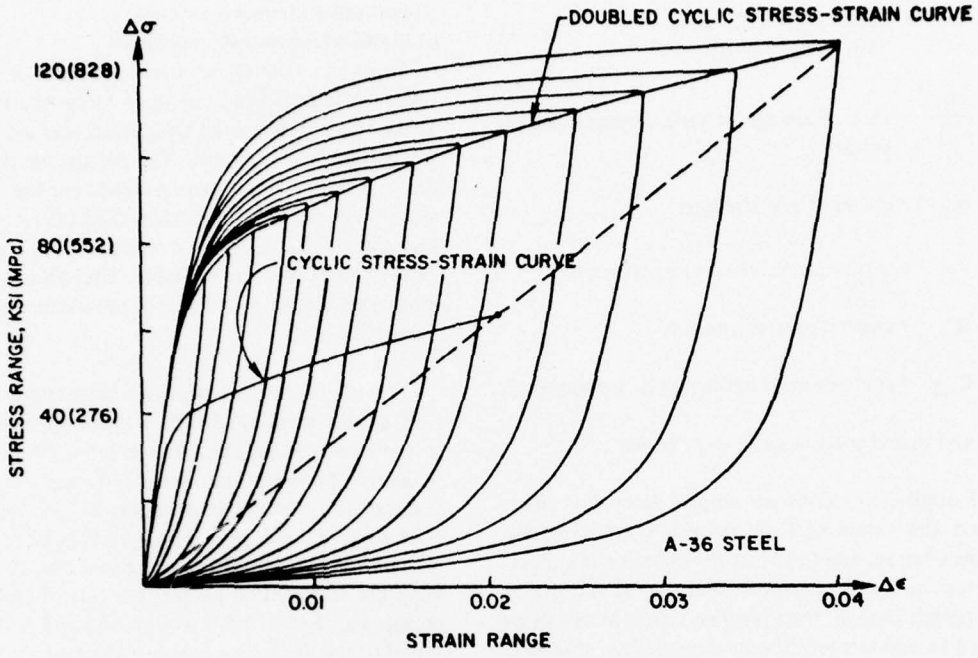

Figure 14. Saturation hysteresis loops of A-36 steel superimposed on their lower tips.

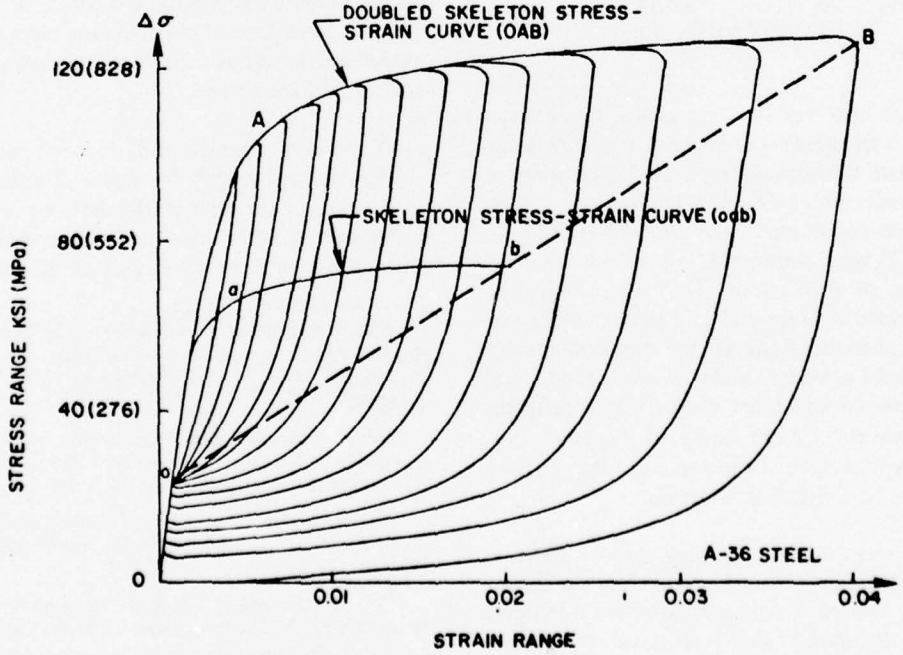

Figure 15. Saturation hysteresis loops of A-36 steel superimposed on lower tips and translated along elastic slope to match nonlinear portions of upper branches.

$$\frac{d\sigma_y}{dR} = C_{HS} \frac{(\sigma_{ys} - \sigma_y)^m}{R^p} \qquad \text{[Eq 1]}$$

where $\frac{d\sigma_y}{dR}$ = rate of change of yield strength per reversal

σ_y = current yield strength

σ_{ys} = saturation value of yield strength

R = current reversal number

C_{HS} = coefficient of hardening or softening

and m and p are suitable exponents.

Eq 1 applies to a constant amplitude cycling situation, and the values of C_{HS}, m, and p are generally functions of strain amplitude. If the equation is expected to yield both the magnitude and sign of the rate of yield strength change, then possible values of m will be restricted to odd integers. If only magnitude is obtained, then such a restriction of the possible value of m is not necessary. By integrating the above equation, an equation relating yield strengths and number of reversals can be obtained as in Eq 2:

$$\int_{\sigma_{y1}}^{\sigma_{ys}} \frac{d\sigma_y}{(\sigma_{ys} - \sigma_y)^m} = C_{HS} \int_1^R \frac{dR}{R^p} \qquad \text{[Eq 2]}$$

To examine how well Eq 2 represents the observed behavior for a specified set of m and p, it is only necessary to evaluate the left- and right-hand expressions at various reversals and to examine the linearity of their relationship on an x-y plot. Four values of m and p (0, 1/2, 1, and 2) were considered, which resulted in 16 combinations for examination. The best combination varied from material to material and between strain levels for each material; however, the one combination which provided a consistent and reasonably good representation between the three materials and different strain levels was m = 1/2 or 1, and p = 1. Figures 16, 17, and 18 are typical plots of expressions of the equation for m = 1, p = 1 for the three materials.

From the above analysis, it is reasonable to assume that under constant strain amplitude cycling, the change rate of yield strength is proportional to the difference between the saturation and current values of yield strength, and inversely proportional to the number of reversals.

Quantitative Characterization of Plastic Hysteresis Phenomena

To obtain a complete characterization of the various transient phenomena, one must know the variation of YRI (or yield strength) both from reversal to reversal and within each reversal. The discussion presented in the previous section provides a basis for the former variation; however, it is relatively difficult to measure the variation of YRI within a given reversal, and no such experimental data are available. Therefore, a physically motivated intuitive model will be assumed for the latter variation.

The number of reversals is a meaningful variable as long as the strain amplitude is constant. For example, in the most general variable strain amplitude situation, in which the strain amplitude differs from reversal to reversal, the number of reversals at each strain amplitude never exceeds one. Thus, number of reversals loses significance as an influencing variable. Therefore, to keep the formulation simple, the rate of yield strength change (or that of YSI) will be assumed to be proportional to the difference between the saturation and current values of yield strength (or that of YSI). The saturation YSI will be assumed to be a unique function of strain amplitude and independent of prior cyclic history. Furthermore, the coefficient of hardening/softening (C_{HS}) will be assumed to be a material constant. Although these assumptions will lead to a somewhat inaccurate prediction of the transient rates, the resulting model will be simple, and it will always approach the correct saturation state.

Dislocation theories and observed stored energy changes in cold work[26-29] suggest that the initial part of a reversal after prior plastic deformation and strain hardening should be associated with some recovery (or slight softening); the latter part of the reversal where

---

[26] R. L. Segall and J. M. Finney, "The Relation Between Physical Properties and the Observed Dislocation Distribution in Fatigued Metals," *Acta Metallurgica*, Vol II (July 1963), pp 685-690.

[27] L. M. Clarebrough, M. E. Hargreaves, and M. H. Loretto, *Changes in Internal Energy Associated With Recovery and Recrystallization of Metals* (Interscience, 1963), pp 63-121.

[28] G. R. Halford, *Stored Energy of Cold Work Changes Induced by Cyclic Deformation*, Ph.D. Thesis (University of Illinois, 1966).

[29] A. S. Iyer and P. Gordon, "Note on the Changes in Stored Energy Produced by Reversals of Deformation," *Transactions of Metallurgical Society of American Institute of Mining, Metallurgical, and Petroleum Engineers*, Vol 52 (1952), pp 1086-1097.

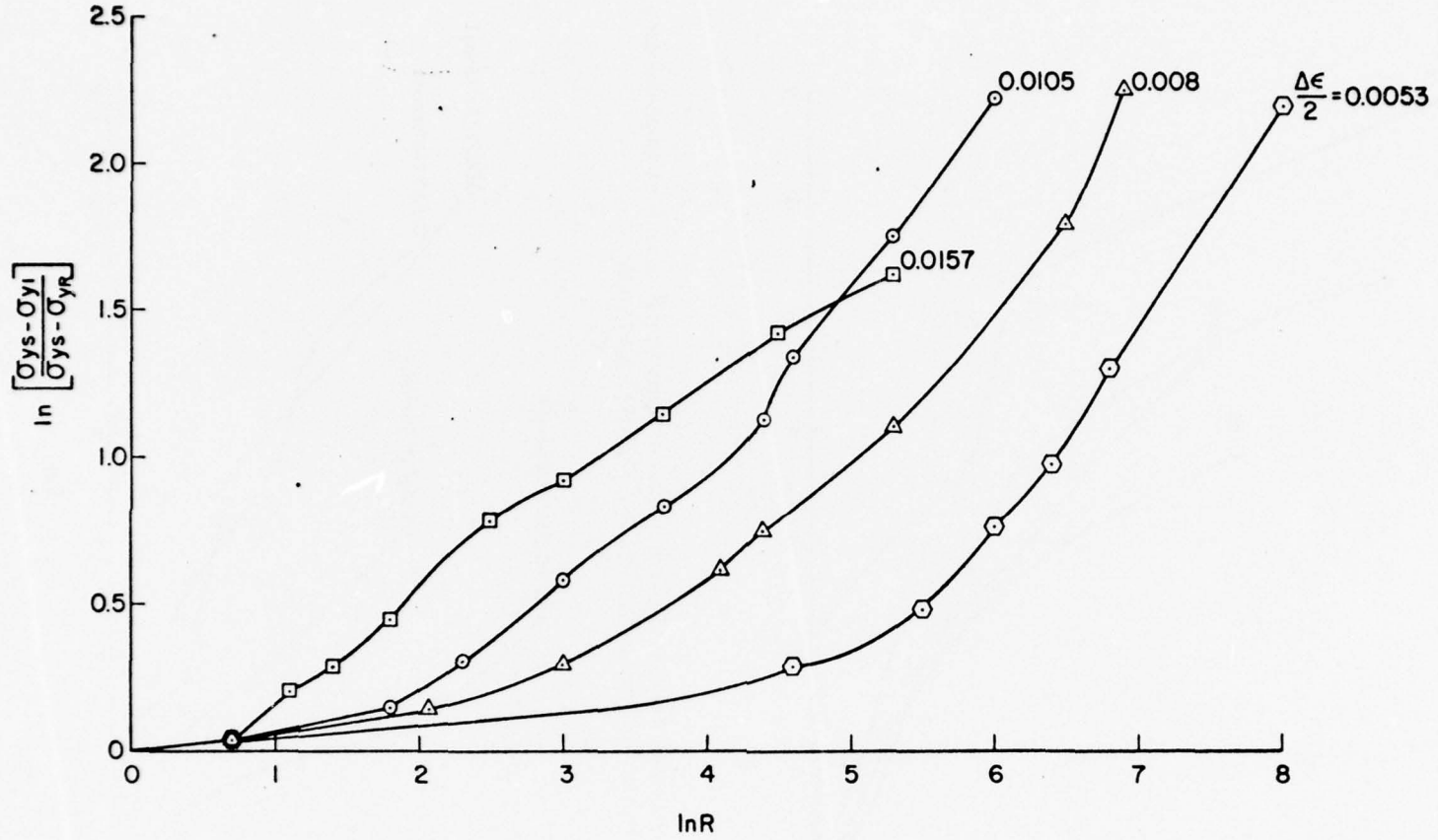

Figure 16. Observed relationship between YRIs and number of reversals of constant strain amplitude during cyclic hardening of 2024-T4 aluminum.

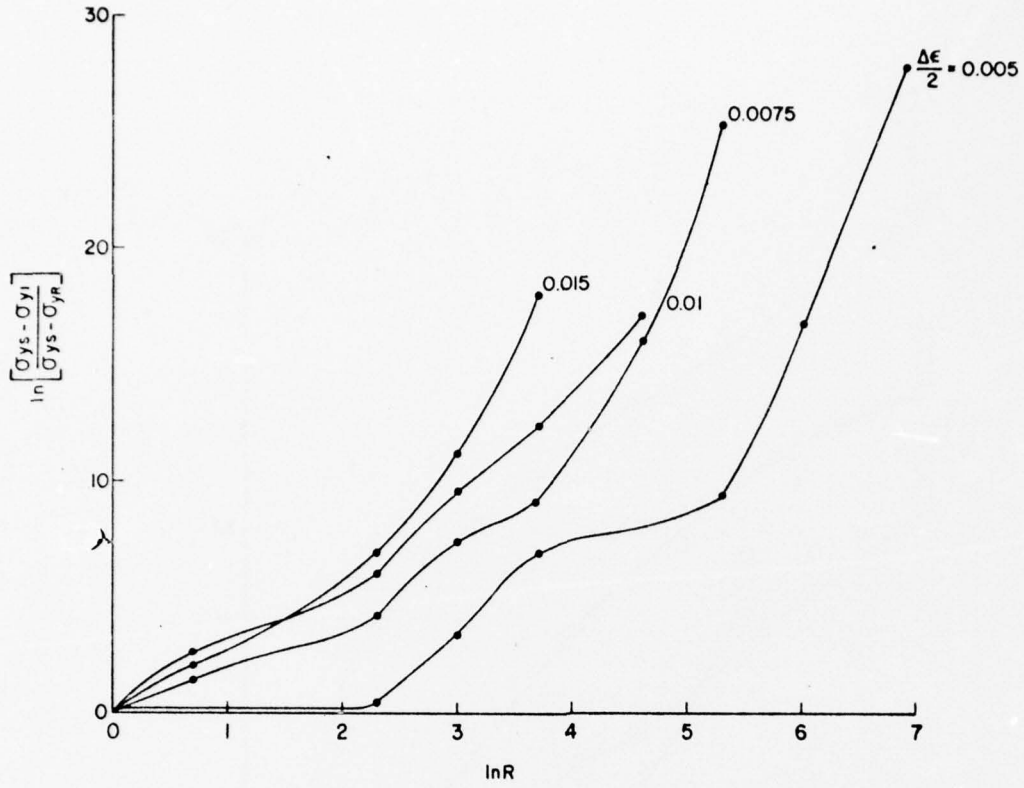

Figure 17. Observed relationship between YRIs and number of reversals of constant strain amplitude during cyclic softening of SAE 1045 quenched and tempered (720°F [328°C]) steel.

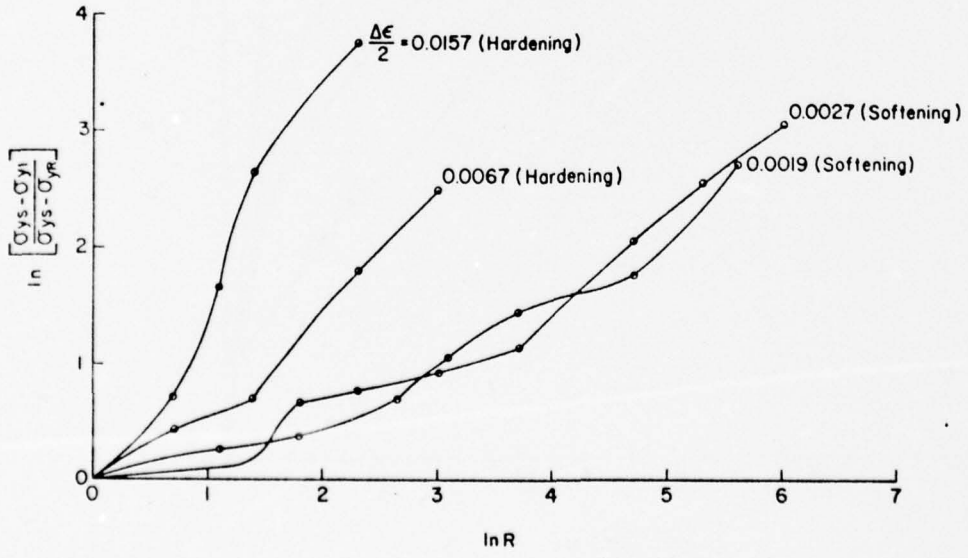

Figure 18. Observed relationship between YRIs and number of reversals of constant strain amplitude during cyclic hardening/softening of SAE 1045 normalized steel.

reversed plastic deformation occurs should be associated with work hardening. This means that the yield strength (or YSI) would initially decrease and then increase in a reversal as reversed plastic deformation takes place. Adopting this view, Figure 19 shows a conceptual cyclic variation of the yield strength under constant amplitude cyclic hardening, cyclic softening, and cyclic saturation conditions. To use a simple quantitative characterization, the variation of YSI within each reversal is assumed to be as shown in Figure 20. During the initial "linear" elastic portion, the YSI is assumed to remain unchanged. At the end of the "linear" elastic part, the YSI is assumed to suddenly reduce by a small fraction of the reversal. The fraction C_{RC} by which the YSI decreases at the end of the elastic part is designated as coefficient of cyclic relaxation/creep and is assumed to be a material constant. During the latter part of the reversal, the YSI is assumed to increase linearly with stress. The value of YSI at the end of the reversal is determined by the model for reversal to reversal variation in YSI discussed in the previous paragraph. The resulting expressions for the YSI at any given point in the reversal are listed in Figure 20. These represent the initial YSIs for the subsequent reversal if the loading direction is changed at the current position of the present reversal. The stress-strain path in each reversal is completely determined by the initial YSI of that reversal. Thus, a characterization of the transient phenomena requires two material constants (C_{HS} and C_{RC}), the determination of which will be discussed in Chapter 4.

It is therefore possible to quantitatively characterize the various cycle-dependent transient phenomena and the observed deviation of real materials from Masing behavior in terms of a single history-dependent parameter—the YSI. This approach has a reasonable physical basis, since the YSI represents the history-dependent variation in the internal friction stress of the material caused by microstructural changes due to cyclic plastic straining.

4 DETERMINATION OF MATERIAL PROPERTIES

Depending on the number of features to be incorporated, development of a cyclic stress-strain reponse model as discussed in the previous two chapters requires some or all of the following properties:

1. Monotonic stress-strain curve
2. Skeleton stress-strain curve
3. First reversal YRI (or YSI) expressed as a function of monotonic strain
4. Saturation YRI (or YSI) expressed as a function of strain amplitude
5. Coefficient of cyclic hardening/softening
6. Coefficient of cyclic relaxation/creep.

The first property—the monotonic stress-strain curve—is obtained from an ordinary tensile test. Since nominal strains exceeding approximately 0.02 are not of interest in structural analysis, the stress-strain curve expressed in engineering units (based on original specimen dimensions) is adequate. The rest of the properties can be termed "cyclic" properties which require special cyclic tests.

Cyclic Tests

Two types of cyclic tests are of interest in determining cyclic properties:

1. Fully reversed constant amplitude tests
2. A multiblock decremental step test.

In both of these tests, a uniaxial specimen is subjected to axial strain cycling between fully reversed specified limits, and the asssociated stress-strain response is recorded on an X-Y recorder. The specimen design, its preparation, and the procedures for testing are described in the forthcoming ASTM standards[30] and a currently available ASTM publication.[31] Therefore, such details are omitted here.

In the case of fully reversed constant strain amplitude tests, several identical specimens are strain-cycled, each at a different strain amplitude. Although it is sufficient to cycle the specimens until saturation is reached, continued cycling to fatique fracture yields additional valuable information for establishing fatigue properties. Since a real test may never reach an ideal state of sat-

[30] *Recommended Practice of Constant Amplitude Low Cycle Fatigue Testing*, Forthcoming ASTM Standards, Part 10 (ASTM).

[31] *ASTM Manual on Low Cycle Fatigue and Testing*, ASTM STP 465 (ASTM, 1969).

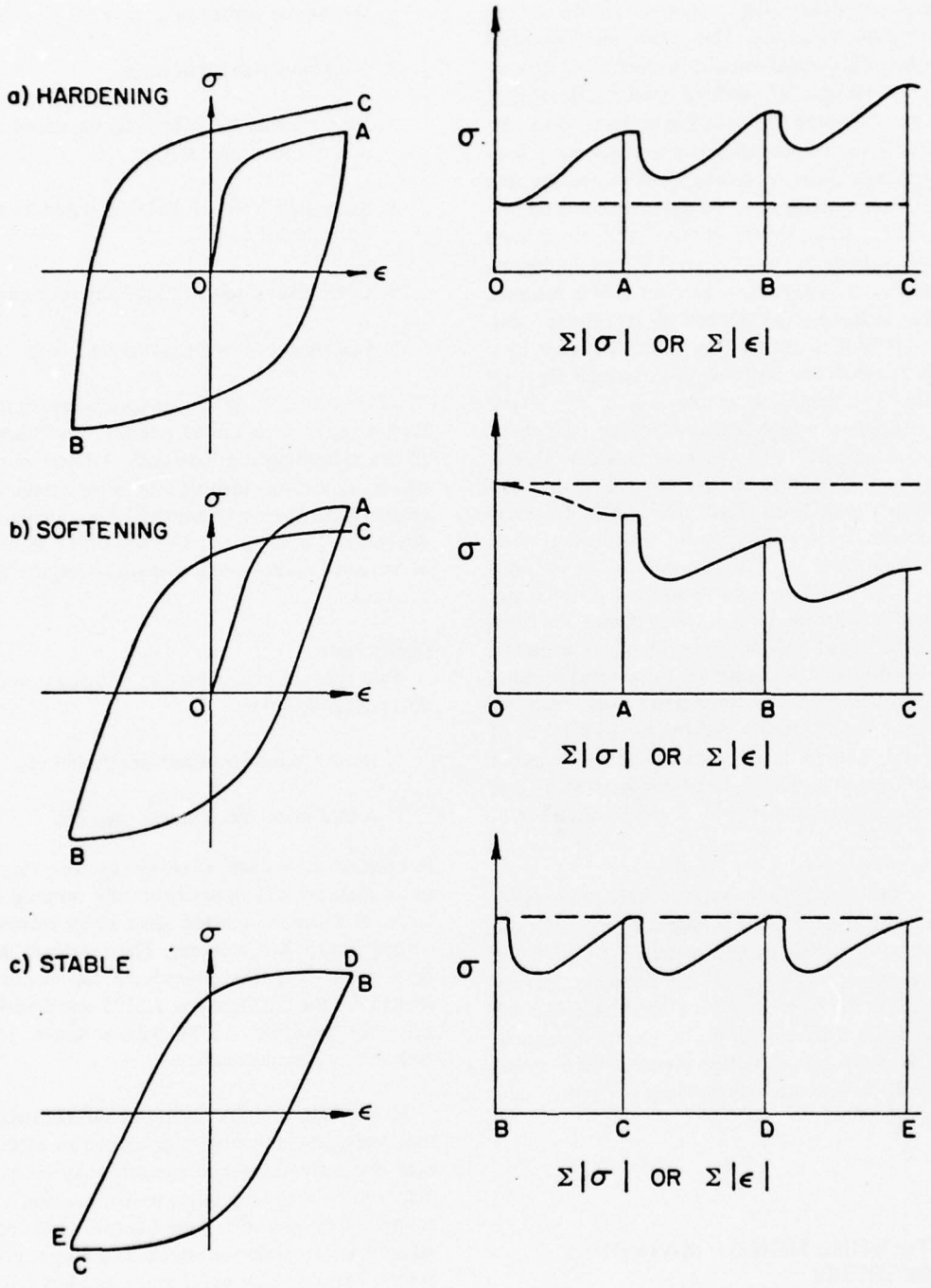

Figure 19. Schematic cyclic variation of yield strength (or YSI or YRI) during cyclic hardening, softening, and saturation states.

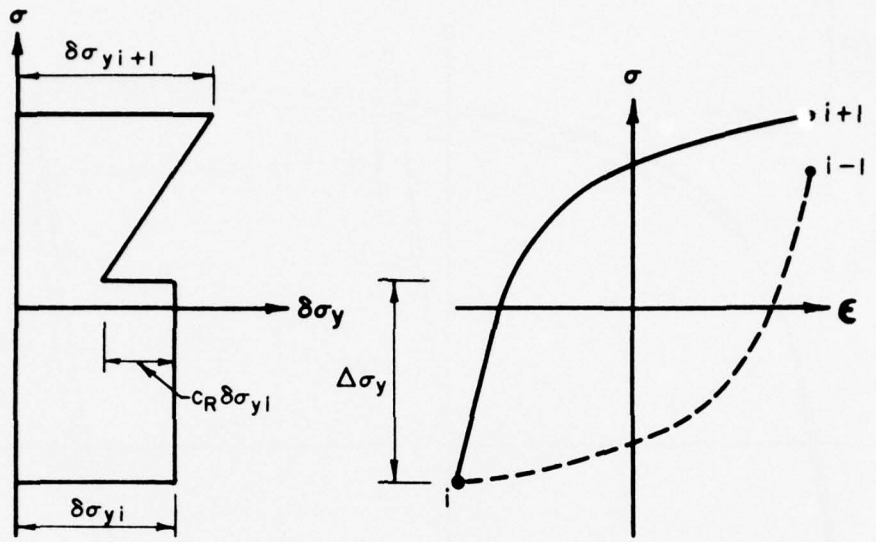

$$\delta\sigma_{yi+1} = \delta\sigma_{yi} + c_H\,(\delta\sigma_{ysi} - \delta\sigma_{yi})$$

Let $\Delta\sigma = |\sigma - \sigma_i|$

$\delta\sigma_y = \delta\sigma_{yi}$ for $\Delta\sigma < \Delta\sigma_y$

$\delta\sigma_y = (1 - c_R)\,\delta\sigma_{yi}$ for $\Delta\sigma = \Delta\sigma_y$

$$\delta\sigma_y = (1 - c_R)\,\delta\sigma_{yi} + [(c_R - c_H)\,\delta\sigma_{yi} + c_H\delta\sigma_{ysi}] \cdot \left|\frac{\sigma}{\sigma_i}\right| \text{ for } \Delta\sigma > \Delta\sigma_y$$

where $\Delta\sigma_y$ = elastic stress range

$\delta\sigma_{ysi}$ = saturation yield strength of range i − 1 to i

c_H = coefficient of cyclic hardening or softening

c_R = coefficient of cyclic relaxation or creep

$\delta\sigma_y$ = yield strength increment

Figure 20. A simple model for the cyclic variation of yield strength (or YSI).

uration, such a condition may be defined as corresponding to minimal changes in the stress-strain hysteresis loops. In some cases, the stage corresponding to one-half of the fatigue life has been adopted as the state of saturation.[32, 33] Figure 21 shows a typical record of stress-strain hysteresis response obtained for A-36 steel during the first four cycles. Since changes in the hysteresis paths are significant during the first few cycles, a continuous record is obtained during these cycles. As cycling continues, it is adequate to record hysteresis loops at logarithmic increments of cycles or reversals.

Figure 22 illustrates a typical strain history imposed in a multiblock decremental step test. A single specimen is strain-cycled at various strain amplitudes, starting from the largest magnitude. At each strain amplitude, the cycling is continued until saturation is achieved at that level and the saturated hysteresis loop is recorded on an X-Y recorder. The next lower strain amplitude level is attained by continuous decrements, as illustrated in Figure 22. Thus, it is possible to obtain saturated hysteresis loops corresponding to several strain amplitudes

[32] R. W. Landgraf, *Cyclic Deformation and Fatigue of Hardened Steels*, T&AM Report 320 (University of Illinois, 1968).

[33] S. Keshavan, *Some Studies on the Deformation and Fracture of Normalized Steel Under Cyclic Conditions*, Ph.D. Dissertation (University of Waterloo, December 1966).

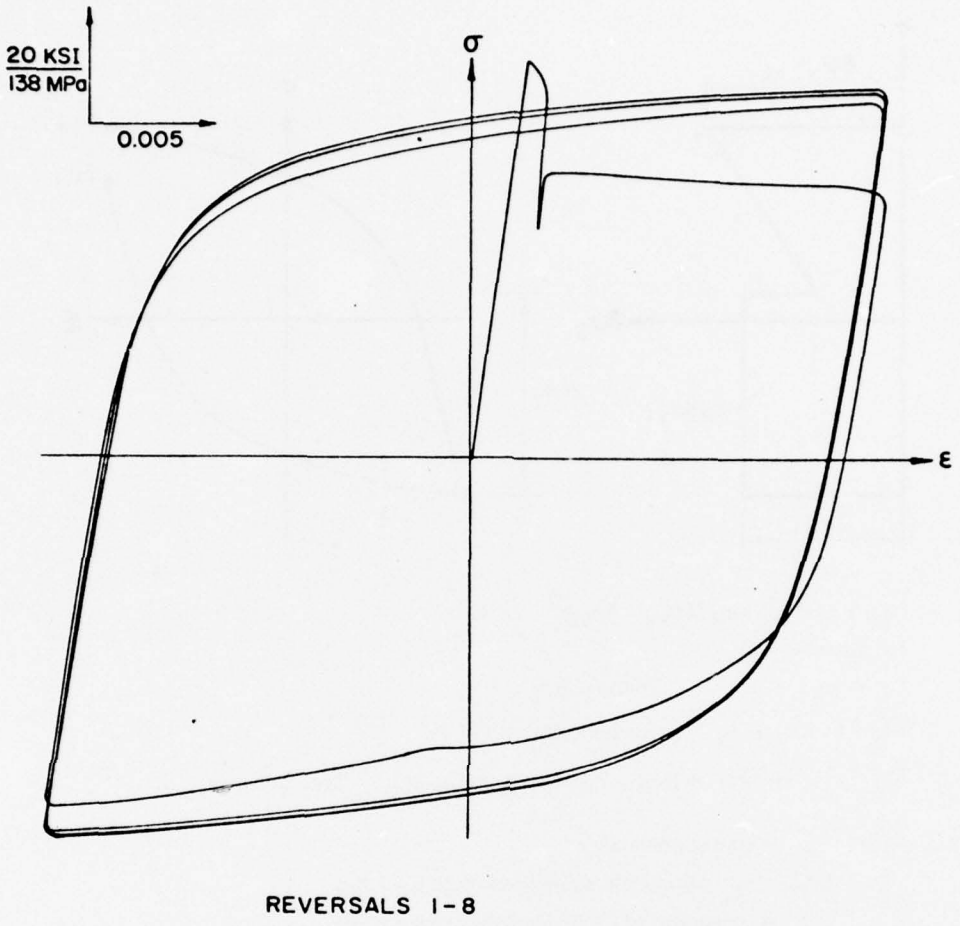

Figure 21. Typical record of hysteresis response of A-36 steel under fully reversed constant strain limits cycling.

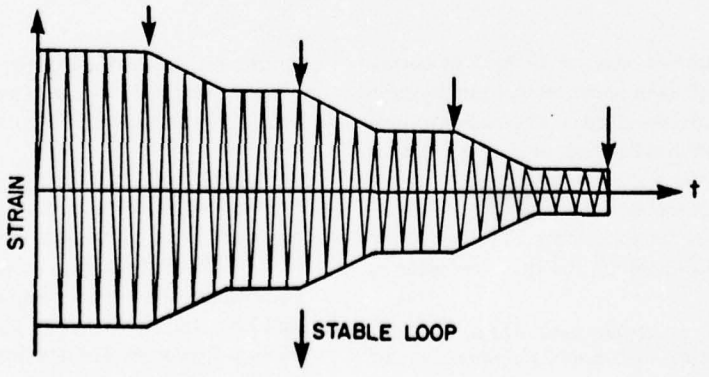

Figure 22. Strain-time history in a multiblock decremental step test.

from a single test; however, this test does not provide any information on the transient properties. In cases where only saturation properties are needed, this test is sufficient to derive all the cyclic material properties.

Determination of Cyclic Properties

Skeleton Stress-Strain Curve

As explained in Chapter 3, the skeleton stress-strain curve is one-half of the invariant portion of a hysteresis branch. Since all the variation caused by transient and non-Masing behavior is associated with the elastic portion, the skeleton stress-strain curve is comprised of the least elastic portion. To determine this, it will be necessary to compare all the first reversal hysteresis branches in the case of cyclic hardening materials, such as 2024-T4 aluminum, and all the saturation hysteresis branches in the case of softening materials, such as cold-formed steels. In the case of materials which exhibit either softening or hardening, it may be necessary to compare both the first reversal and saturation hysteresis branches. However, based on the observation of three normal steels—SAE 1018 normalized steel, SAE 1045 normalized steel, and A-36 steel, all of which exhibit either softening or hardening—it was sufficient to compare the saturation hysteresis branches of these materials to determine the skeleton stress-strain curve.

Figures 14 and 15 illustrate a convenient procedure for determining the skeleton of stress-strain curve from a comparison of the saturation hysteresis branches of A-36 steel. The procedure would be similar in the case of first reversal branches. The various sized hysteresis loops are superimposed on their lower (or upper) tips as shown in Figure 14, and then translated along the elastic slope until all the upper (or lower) branches are matched as well as possible, as shown in Figure 15. Curve OAB defines doubled skeleton stress-strain curve.

It is of interest to note the difference between the skeleton stress-strain curve and the cyclic stress-strain curve defined in low-cycle fatigue literature.[34] The cyclic stress-strain curve is defined as the locus of tips of saturated hysteresis loops, and therefore, the curve joining the locus of branch tips defines the doubled cyclic stress-strain curve. Figure 23 illustrates the difference between the skeleton and the cyclic stress-strain curves for the three types of materials. The difference in stress levels between these two curves at a specified plastic strain level is the saturation YSI corresponding to that plastic strain.

[34] R. W. Landgraf, J. Morrow, and T. Endo, "Determination of the Cyclic Stress-Strain Curve," *Journal of Materials, ASTM-JMLSA*, Vol 4, No. 1 (March 1969), pp 176-188.

When approximating the skeleton stress-strain curve by piecewise linear segments, it is desirable to choose arbitrary lengths for segments in order to accurately represent the curve with a minimum number of segments; this is significant for reducing computational cost. Chapter 5 illustrates two examples of piecewise linear approximation.

First Reversal and Saturation YRIs or YSIs

Since the skeleton stress-strain curve is associated with the least elastic portion, by definition, the YSI corresponding to the skeleton curve is zero; hence, YRI (or YSI) corresponding to any other hysteresis branch is always positive. The YRI corresponding to any given hysteresis branch can be determined by measuring the difference in the elastic portions between the hysteresis branch and doubled skeleton stress-strain curve in stress units. As their names indicate, the first reversal and saturation YRIs correspond to those branches. Since each strain amplitude is associated with a first reversal hysteresis and a saturation hysteresis loop, the first reversal and saturation YRIs can be expressed as functions of strain amplitude. Figures 10, 11, and 12 were obtained in this manner.

Coefficient of Cyclic Hardening/Softening

As discussed in Chapter 3, the coefficient of cyclic hardening/softening is generally not only a function of the material but is also dependent on strain amplitude. However, to keep the calculation simple, this coefficient is being treated as a material constant. The following procedure may be used to select a reasonable value for this coefficient. Based on the assumption that the rate of change in yield strength per reversal is proportional to the difference between the saturation and current values of yield strength presented in Chapter 3, the following expression for the coefficient of cyclic hardening/softening, C_{HS}, can be derived.

$$C_{HS} = \frac{\ell n(1-f)^{-1}}{R-1} \qquad \text{[Eq 3]}$$

where f = degree of saturation expressed as a fraction (f = 1 represents complete saturation)

R = number of reversals to reach this degree of saturation under constant strain cycling.

For example, to achieve a 90 percent saturation in 10 reversals, a $C_{HS} \cong 0.25$ is required. It is possible to

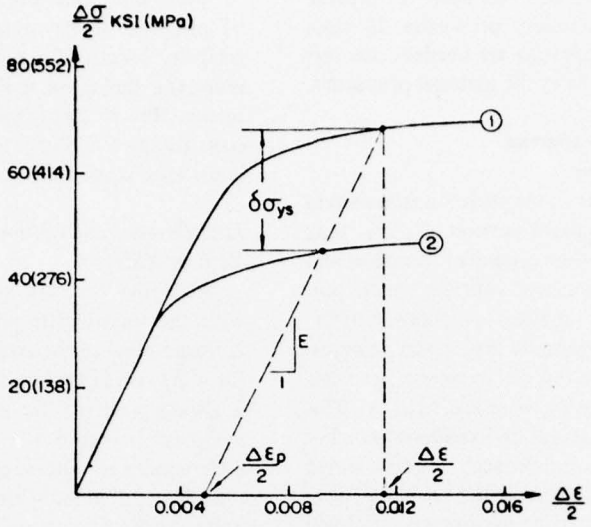

(a) 2024-T4 aluminum

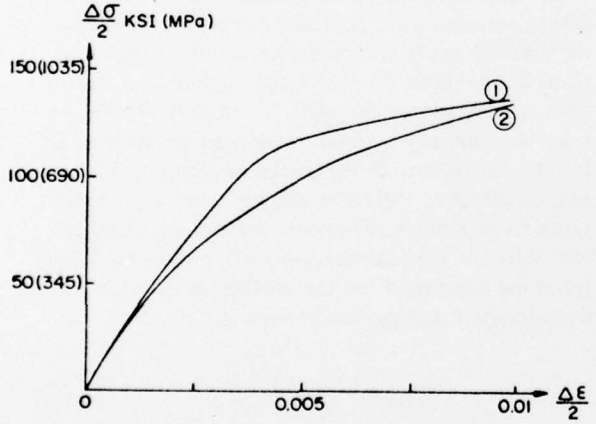

(b) SAE 1045 steel, Q&T (720°F)

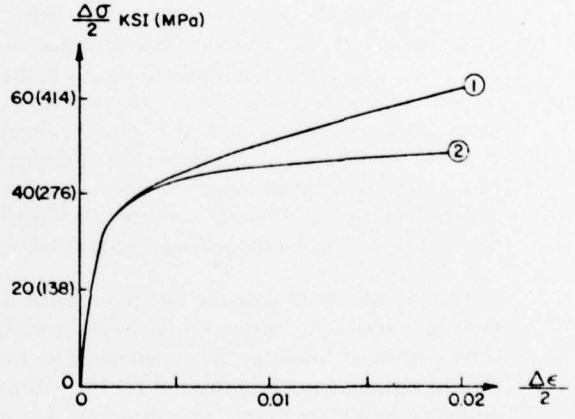

(c) A-36 steel

Figure 23. Comparison between cyclic and skeleton stress-strain curves of three materials (1 = cyclic curve, and 2 = skeleton curve).

pick a reasonable set of f and R values from the observed transient behavior in constant strain cycling tests. In the absence of such data, a reasonable value of C_{HS} based on the observed behavior of three materials (see Chapter 3) appears to be 0.1 to 0.2.

Coefficient of Cyclic Relaxation/Creep

As explained in Chapter 3, there are no quantitative measurements of the degree of recovery on unloading after prior plastic deformation. Thus, knowledge about the coefficient of cyclic relaxation/creep related to this phenomenon is incomplete. A value of 0.1 to 0.5 appears to be reasonable, since the use of such a value in a model results in a qualitatively reasonable simulation of observed cyclic relaxation/creep behavior of A-36 steel and 2024-T4 aluminum (see Chapter 5).

Therefore, the various material parameters (or properties) required by the inelastic response model can be determined from a set of simple cyclic uniaxial tests of constant strain amplitude.

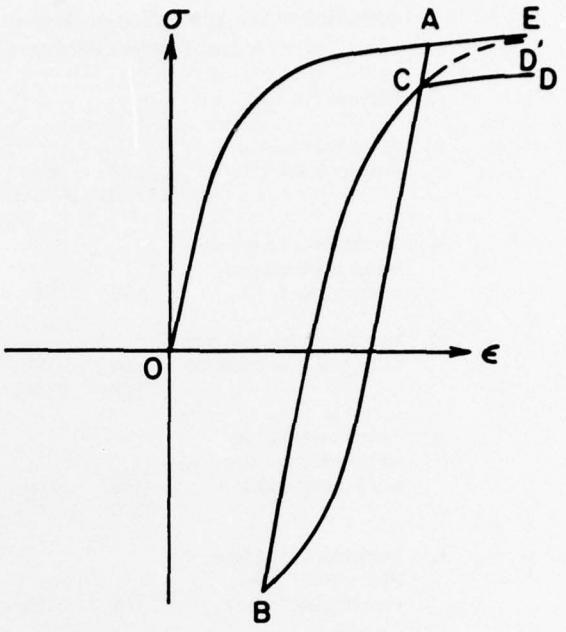

Figure 24. Effect of relaxation on memory phenomenon.

5 MODELING CYCLIC STRESS-STRAIN RESPONSE

This chapter discusses three aspects of the model for cyclic stress-strain response:

1. Development of a model to simulate both memory and plastic hysteresis phenomena
2. Degrees of approximation/simplification in the model and appropriate areas of application
3. Typical simulations of two different materials' behavior.

Combined Model for Memory and Plastic Hysteresis Phenomena

The memory model presented in Chapter 2 can be simply modified to incorporate the transient and non-Masing characteristics of real materials by varying the length of the first linear segment of the stress-strain curve as denoted by the variation in YSI. The model for the history-dependent variation of YSI was discussed in Chapter 3. The basic length and slope of the first segment and the lengths and slopes of other segments are defined by the skeleton stress-strain curve and are therefore history-independent material constants.

In addition to the above modification, it is necessary to modify the memory rules slightly for the availabilities of certain segments during relaxation/creep to properly simulate observed material behavior. Figure 24 illustrates this problem for the case of relaxation. The difference between the branches AB and BC is due to YRI of BC being less than YRI of AB. If loading is continued beyond C, the memory model (or rules) will describe a path CD parallel to AE, which is a continuation of OA; however, real materials follow a path similar to CD.[35] Although this appears to be a minor discrepancy in the example illustrated, it will cause significant errors in the simulation of cyclic creep.

The observed material behavior can be simulated by recovering the availabilities of those segments that are either partially available or totally unavailable to the extent of decrease in YRI. The following additional memory rules (memory rule 5) is added to those presented in Chapter 2.

[35] H. R. Jhansale, *Inelastic Deformation and Fatigue Response of Spectrum Loaded Strain Controlled Axial and Flexural Members*, Ph.D. Dissertation (University of Waterloo, 1961).

Table 2
Illustration of the Application of Memory Rule 5 to the Simulation Example for Figure 27(a) for the Last Reversal Between Strain Limits +0.01 and +0.02 (A-36 Steel)

i	Segment No.	1	2	3	4	5	6	7	8
A_i	Stress increment of segment in ksi (MPa)	20.00 (137.90)	10.00 (68.95)	5.00 (34.47)	5.00 (34.47)	5.00 (34.47)	2.50 (17.24)	1.00 (6.89)	1.50 (10.34)
B_i	Availability of segment before application of memory rule 5	2.00	2.00	2.00	2.00	1.73	0.00	0.00	0.95
C_i	Maximum stress that can be recovered in ksi (MPa)	0.00 (0.00)	0.00 (0.00)	0.00 (0.00)	0.00 (0.00)	1.35 (9.31)	5.00 (34.47)	2.00 (13.79)	1.575 (10.859)
D_i	Actual stress that is recovered as per memory rule 5, in ksi (MPa)	0.00 (0.00)	0.00 (0.00)	0.00 (0.00)	0.00 (0.00)	0.49 (3.38)	0.00 (0.00)	0.00 (0.00)	0.00 (0.00)
E_i	Availability of segment after application of memory rule 5	2.00	2.00	2.00	2.00	1.83	0.00	0.00	0.95

Legend: Given A_i, B_i, and ΣD_i, which is the total amount of relaxation between previous and current reversals, the quantities C_i, D_i, and E_i are calculated from the following equations:

1. $C_i = (2.00 - B_i) \cdot A_i$
2. $D_i \leq C_i$
3. $\sum_{i=1}^{8} D_i = 0.49$ (Known)
4. $E_i = B_i + D_i/A_i$

If transient features are simulated, and if the YRI at the beginning of the current reversal is less than that at the beginning of the previous reversal, the availability coefficients of the segments associated with the current reversal are increased as follows. Starting with the first, and in consecutive order, the availability coefficients of as many segments as required are increased so that the total sum of increases in stress increments is equal to the difference in YRIs between the beginning of the previous and current reversals. The increase in availability coefficients for each segment is limited by the condition that the availability coefficient does not exceed *two* in conformity with memory rule 2. The availability coefficients of segments corresponding to opposite direction are appropriately reduced. The application of this rule is illustrated in Table 2 for the last reversal of the example presented in Figure 27a, which is described in the section **Typical Models and Simulation for Two Materials**.

The monotonic stress-strain curves of softening and strain-aging materials are different in shape from the rest of the hysteresis branches described by the skeleton stress-strain curve. Therefore, to simulate the initial monotonic path accurately, it is necessary to initially assign the various segments of the stress-strain curve; it is then necessary to change these values to those given by the skeleton stress-strain curve at the end of monotonic loading.

Approximations and Appropriate Applications

Whereas a model capable of simulating all the observed material phenomena is generally useful, simplifi-

Table 3
Possible Degrees of Approximation/Simplification in Modeling
Material Behavior and Appropriate Applications

Model/Degree of Approximation	Material Features That Can Be Simulated[a]	Material Properties That Are Needed and the Minimum Number of Material Characterization Tests[b]	Application(s) Which Require This Model
1	All four features: A to D	All six properties: 1 - 6 Number of tests: 6 - 8	Deformation analyses with relatively few cycles of inelastic loads.
2	Features: B to D	Properties: 3 to 6 Number of tests: 2	Deformation analyses with several cycles of loading. Fatigue analysis where mean stress effect is important.
3	Features: C & D	Properties: 5 & 6 Number of tests: 1 - 2	Deformation analysis where transient behavior is unimportant. Fatigue analysis involving non-Masing materials where mean stress effect is not important.
4	Feature D only	Cyclic stress-strain curve Number of tests: 1	Same as for model 3, except the application is limited to Masing materials.

[a]**Material Features:** *A. Initial cyclic hardening/softening; B. transient behavior due to irregular cyclic loading;* C. stable non-Masing behavior; and D. stable Masing behavior.

[b]**Material Properties:** 1. Monotonic stress-strain curve; 2. first reversal of yield strength increment; 3. coefficient of cyclic hardening/softening; 4. coefficient of cyclic relaxation/creep; 5. skeleton stress-strain curve; and 6. saturation yield strength increment or cyclic stress-strain curve.

cations or approximations may still provide adequate models for certain applications. From the point of view of such simplifications, the observed material phenomena discussed and analyzed in the previous chapters can be divided into four features:

1. Initial cyclic hardening or softening

2. Transient behavior due to irregular cyclic loading which includes combined cyclic hardening or softening and cyclic relaxation or creep (see Chapter 3)

3. Memory phenomenon with non-Masing characteristics

4. Memory phenomenon with Masing characteristics.

Four models which include three degrees of simplification result from the above categorization, as shown in Table 3. Model 1 is capable of simulating all the four material features described above and is therefore generally useful for all applications listed in the last column of Table 3. Models 2, 3, and 4 correspond to increasing degrees of approximation or simplification. Model 2 ignores the initial cyclic hardening or softening feature, and the material is not assumed to be initially at the state of saturation. Models 3 and 4 are not capable of simulating transient behavior. Although mean stresses are important in some situations, transient phenomena are not usually considered to be significant in cumulative fatigue damage analysis. Therefore, models 3 and 4 would be adequate for use in fatigue analysis problems, where mean stress effect is not important.

Table 3 also lists the required material properties and the number of tests to determine the properties of each model. Obviously, model 1 requires all six properties (see Chapter 4) and the other models require only some of these properties. It is of interest to note that the number of material characterization tests required to formulate model 2 are about the same as those for

models 3 and 4, but model 2 is much superior to models 3 or 4. Also, to improve from model 2 to model 1, a considerable increase in the material characterization tests is needed.

Typical Models and Simulation for Two Materials

The distinguishing transient behavior features of 2024-T4 aluminum and A-36 steel will be illustrated by appropriate models for these two materials. Figure 25 illustrates the observed cyclic relaxation behavior of 2024-T4 aluminum and a mild steel (which is similar to A-36 steel) under strain cycling conditions in the presence of a mean stress. The 2024-T4 aluminum exhibits a simultaneous cyclic hardening, whereas the mild steel (and strain-aging structural steels in general) exhibits a simultaneous cyclic softening in addition to cyclic relaxation. These phenomena appear as cycle-dependent increases or decreases in stress range, respectively, as shown by the figure. This difference can be attributed to the different in the saturation YSI properties between the two materials; this will be demonstrated by model simulation.

2024-T4 Aluminum

Using the model 1 degree of sophistication, Table 4 lists the required material properties. In the case of 2024-T4 aluminum, the monotonic and skeleton stress-strain curves are identical. The first reversal YSI and saturation YSI are constants and independent of strain amplitude. For illustration, the skeleton stress-strain is approximated by nine linear segments; the coefficients of cyclic hardening/softening and coefficient of cyclic relaxation/creep are chosen as 0.1.

Figure 26 shows the simulated stress-strain response of 2024-T4 aluminum for a specified input strain history. Figure 26a illustrates cyclic hardening during the first eight reversals of strain amplitude, $\frac{\Delta\epsilon}{2} = 0.012$, and Figure 26b illustrates the combined cyclic relaxation and hardening in the presence of a tensile mean stress.

A-36 Steel

Adopting the model 2 formulation for this case, the initial cyclic softening or hardening feature is neglected; i.e., the material is assumed to be in the saturated condition initially. The initial monotonic stress-strain path is, therefore, given by the cyclic stress-strain curve. Table 5 lists the material properties required for this formulation. Only two properties the skeleton stress-strain curve and the cyclic stress-strain curve need to be known,

Table 4
Cyclic Material Properties of 2024-T4 Aluminum for Model 1

1. Monotonic stress-strain curve is the same as skeleton stress-strain curve.

2. Skeleton stress-strain curve (piecewise linear approximation).

Node	Stress, ksi (MPa)	Strain
1	0.0 (0.0)	0.0
2	30.0 (206.9)	0.003
3	35.0 (241.3)	0.0037
4	40.0 (275.8)	0.0050
5	42.5 (293.0)	0.006
6	45.0 (310.3)	0.0073
7	47.5 (327.5)	0.0098
8	48.75 (336.13)	0.011
9	50.0 (347.5)	0.0131
10	51.2 (353.0)	0.0153

3. First reversal YSI = 0.0 ksi (0.0 MPa).

4. Saturation YSI = 25.0 ksi (172.4 MPa).

5. Coefficient of cyclic hardening/softening = 0.1.

6. Coefficient of cyclic relaxation/creep = 0.1.

Table 5
Cyclic Material Properties of A-36 Steel for Model 2

1. Skeleton stress-strain curve (piecewise linear approximation)

Node	Stress, ksi, MPa	Strain
1	0.0 (0.0)	0.0
2	20.0 (137.9)	0.0007
3	30.0 (206.9)	0.0013
4	35.0 (241.3)	0.0017
5	40.0 (275.8)	0.0027
6	45.0 (310.3)	0.0053
7	47.5 (327.5)	0.0092
8	48.5 (334.4)	0.015
9	50.0 (347.5)	0.03

2. Saturation YSI ($\delta\sigma_{ys}$) in ksi expressed as a function of plastic strain amplitude ($\Delta\epsilon p/2$):

$$\delta\sigma_{ys} = 1745 \times \frac{\Delta\epsilon p}{2}, \text{ for } \frac{\Delta\epsilon p}{2} < 0.002.$$

$$\delta\sigma_{ys} = 620 \times \frac{\Delta\epsilon p}{2} + 2.25, \text{ for } 0.002 \leq \frac{\Delta\epsilon p}{2} < 0.0045.$$

$$\delta\sigma_{ys} = 291.25 \times \frac{\Delta\epsilon p}{2} + 3.73 \text{ for } 0.0045 \leq \frac{\Delta\epsilon p}{2} < .011.$$

$$\delta\sigma_{ys} = 5.55 \times \frac{\Delta\epsilon p}{2} + 7.5 \text{ for } \frac{\Delta\epsilon p}{2} \geq 0.011.$$

3. Coefficient of cyclic hardening/softening = 0.1.

4. Coefficient of cyclic relaxation/creep = 0.3

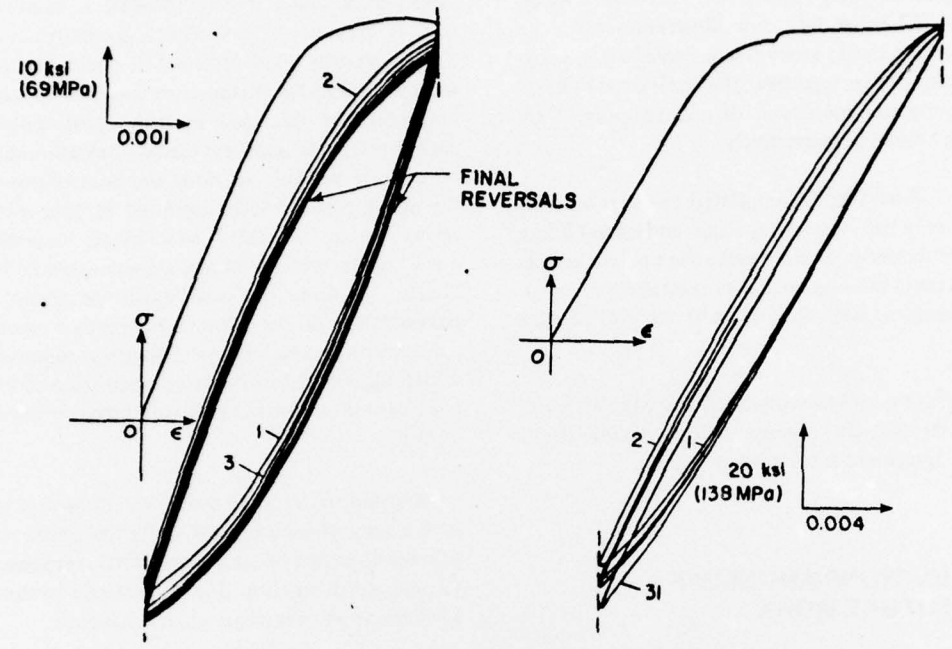

(a) Combined cyclic relaxation and softening of mild steel under constant strain cycling.

(b) Combined cyclic relaxation and hardening of 2024-T4 aluminum.

Figure 25. Cyclic relaxation behavior of 2024-T4 aluminum and mild steel.

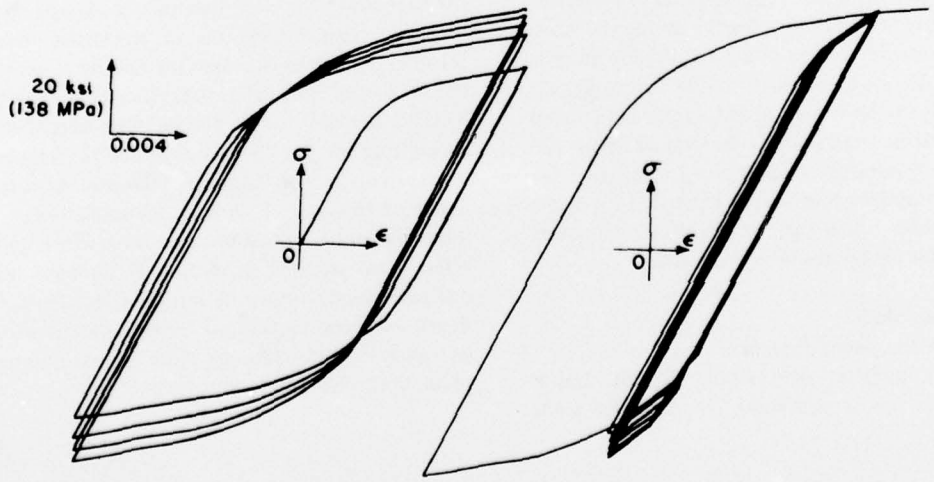

(a) Cyclic hardening.

(b) Combined cyclic relaxation and hardening.

Figure 26. Simulation of cyclic hardening and combined cyclic relaxation and hardening of 2024-T4 aluminum under strain cycling history: (1) 0 to 0.012, one to eight reversals at ±0.012 and (2) nine to ten reversals at ±0.012, one to nine reversals at +0.012 and −0.002 and one reversal at −0.002 and +0.015.

since the third property (saturation YSI) can be determined from the other two. For illustration, both the skeleton and the cyclic stress-strain curves are approximated by eight linear segments; the coefficient of hardening/softening and coefficient of relaxation/creep are chosen as 0.1 and 0.3, respectively.

Figure 27 illustrates the simulated cyclic relaxation and cyclic creep behavior under strain and stress cycling histories, respectively. In both cases the model exhibits a cyclic softening simultaneous with relaxation or creep, which is consistent with the observed behavior of mild steels.

Figure 28 compares the simulated and experimentally observed stress-strain response under a variable strain history; the agreement is reasonably good.

6 APPLICATIONS AND SCOPE FOR FUTURE WORK

The work presented in this report is directly or indirectly useful in three applications of structural mechanics and failure analysis.

Basic Material Parameters for Constitutive Equations

The cyclic material properties developed in this work provide the necessary basic properties for formulating material constitutive equations for the multiaxial stress states. Such constitutive equations are directly adoptable in finite element computer codes for nonlinear structural analysis. As explained in Chapter 1, the need for nonlinear structural analysis techniques in seismic design is well recognized. A plasticity formulation for developing appropriate constitutive equations for cyclic loading conditions which uses the material parameters developed in this report has been proposed.[36]

Direct Hysteresis Model for Structural Component/System

A material's inelastic stress-strain response has a major influence on a structural component's load-deformation characteristic, in addition to other factors such as stress or strain gradients, geometry, or joint slip. The hysteretic load-deformation behavior often has features qualitatively similar to the material stress-strain characteristics discussed in this report. Therefore, in such cases, cyclic inelastic load-deformation models can be directly formulated along the lines of development for the material model outlined in this report. The terms "stress," "strain," and "cyclic material parameters" in the material model are analogous to the terms "load," "deformation," and "cyclic components/system parameters" in the structural response model. The component parameters (or properties) required by the structural model can be determined from simple cyclic tests of components similar to those outlined in this report.

A structural reponse model would be directly useful in the area of seismic analysis; a few applications are: (1) development of accurate inelastic response spectra, (2) energy dissipation due to inelastic hysteresis, and (3) evaluation of realistic ductility factors.

Fatigue Analysis Under Complex Histories

Extensive low-cycle fatigue research during the past two decades has shown that the fatigue process consists of an initial crack initiation stage and a final crack propagation stage. The stress and plastic strain fields in a structure's critical locations govern the rate of damage during these two stages of fatigue. Therefore, the material model discussed in this report is directly useful for evaluating the accumulation of fatigue damage at specified critical locations of structures, because it provides complete information on the stress-strain response of the material at these locations. However, the inelastic response model plays a more important role in accounting for the "sequence effect" in fatigue, which is essentially a manifestation of the prior history dependence of the rate of damage accumulation.[37] Simple linear damage summation procedures which ignore this effect have resulted in extremely nonconservative or conservative estimates of fatigue lives. Thus, history-dependent inelastic response models would be extremely valuable for achieving more accurate fatigue life prediction procedures.

---

[36] S. K. Sharma and H. R. Jhansale, *A Plasticity Formulation for Cyclic Inelastic Structural Analysis*, Interim Report M-202/ADA037047 (U. S. Army Construction Engineering Research Laboratory, 1977).

[37] H. R. Jhansale, "Evaluation of Deformation Phenomena of Metals for Fatigue Analysis," *Journal of Testing and Evaluation, ASTM-JTEVA*, Vol 3, No. 5 (ASTM, September 1975), pp 348-354.

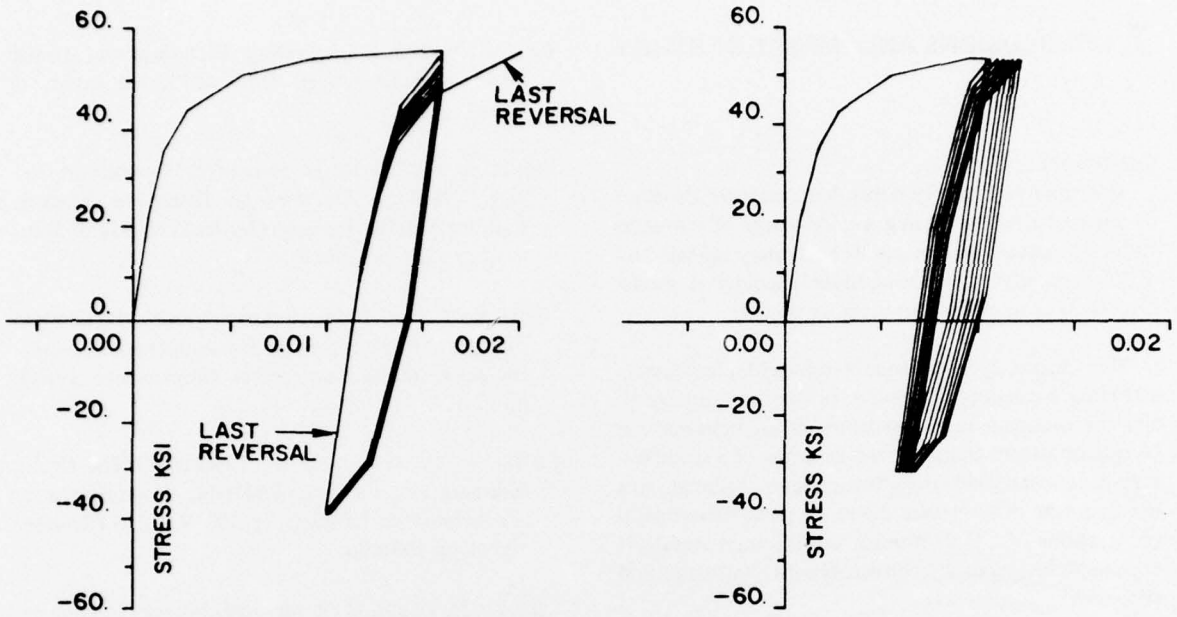

(a) Combined cyclic relaxation and softening under strain cycling between +0.01 to +0.016.

(b) Combined cyclic creep and softening under stress cycling between -32.0 to +54.00 ksi (-220.6 to +372.3 MPa).

Figure 27. Simulation of transient behavior of A-36 steel.

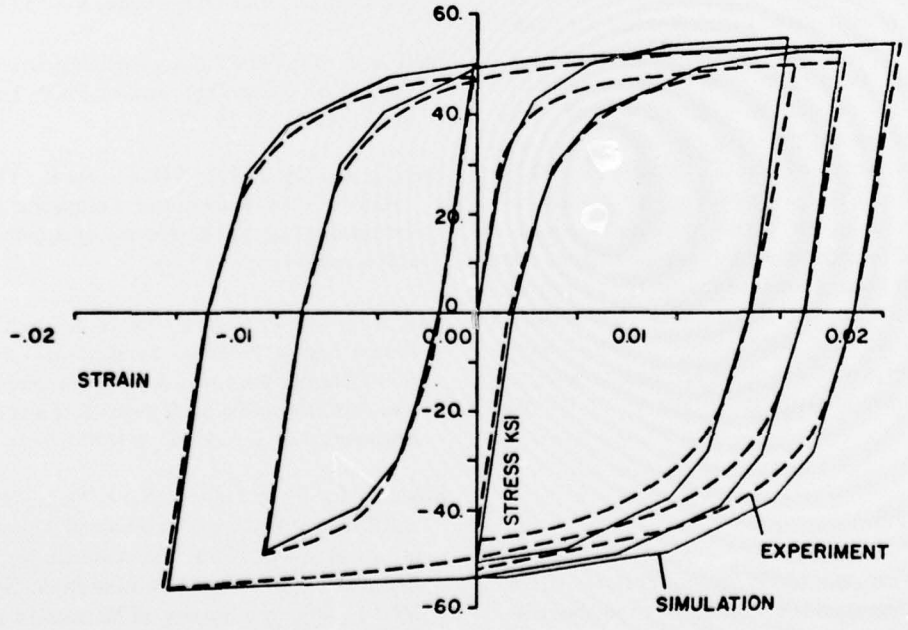

Figure 28. Comparison of simulated and experimentally observed hysteresis behavior of A-36 steel under a variable strain history.

7 CONCLUSIONS AND IMPACT OF STUDY

Conclusions

The observed history-dependent inelastic behavior of structural metals having a wide range of strengths and cyclic characteristics can be accurately modeled by slightly modifying a spring-slider rheological model (Figure 3) or its equivalent memory model.

The various cycle-dependent transient phenomena, including hardening, softening, relaxation, and creep, and the observed deviation from Masing behavior can be quantitatively characterized in terms of a single history-dependent yield strength parameter. Although this development is essentially based on phenomenological observations of a large number of structural metals, it appears to be physically consistent with microstructural processes.

All the material parameters required by the model can be determined from simple cyclic tests of constant strain amplitude.

Impact of Study

This research program has achieved an important step in formulating a nonlinear inelastic structural analysis procedure for such complex loadings as those experienced during earthquakes. Incorporating the developments of this research should make it possible to accurately predict the nonlinear dynamic response of seismic structures; in addition, it should now be possible to evaluate damping coefficients and/or ductility factors used in seismic design (see, for example, TM 5-809-10, *Seismic Design for Buildings*) on a more rational basis than using past experience. Thus, the study has contributed to improvement of seismic analysis and design methods both in terms of reliability and cost effectiveness. Extension of this research into fatigue, fracture, and shakedown problems would provide accurate quantitative procedures for evaluating time-history-dependent cumulative damage criteria under seismic loadings.

REFERENCES

ASTM Manual on Low Cycle Fatigue Testing, ASTM STP 465 (American Society for Testing and Materials [ASTM], 1969).

Berg, G. V. and J. L. Stratha, *Anchorage and Alaska Earthquake* (American Iron and Steel Institute, 1964).

Bresler, B., "Behavior of Structural Elements–A Review," *Building Practices for Disaster Mitigation*, Building Science Series 46 (National Bureau of Standards, 1973), pp 286-351.

Clarebrough, L. M., M. E. Hargreaves, and M. H. Loretto, *Changes in Internal Energy Associated with Recovery and Recrystallization of Metals* (Interscience, 1963), pp 63-121.

Coffin, L. F., Jr., and J. F. Tavernelli, "The Cyclic Straining and Fatigue of Metals," *Transactions of the Metallurgical Society, AIME*, Vol 215 (October 1959), pp 794-806.

Dittmer, D. F. and M. R. Mitchell, *Material Characterization of Cast 8630 Steel: Monotonic and Cyclic Stress-Strain Behavior and Strain-life Response*, FCP Report No. 13 (College of Engineering, University of Illinois, October 1974).

Felter, C. E. and C. Laird, "Cyclic Stress-Strain Response of FCC Metals and Alloys, I-Phenomenological Experiments, II-Dislocation Structures and Mechanisms," *Acta Metallurgica*, Vol 15 (1967).

Halford, G. R., *Stored Energy of Cold Work Changes Induced by Cyclic Deformation*, Ph.D. Thesis (University of Illinois, 1966).

Iwan, W. D., "On a Class of Models for the Yielding Behavior of Continuous and Composite Systems," *Transactions of ASME, Journal of Applied Mechanics* (September 1967).

Iyer, A. S. and P. Gordon, "Note on the Changes in Stored Energy Produced by Reversals of Deformation," *Transactions of Metallurgical Society of American Institute of Mining, Metallurgical, and Petroleum Engineers*, Vol 52 (1952), pp 1086-1097.

Jaske, C. E., B. N. Leis, and C. E. Pugh, "Monotonic and Cyclic Stress-Strain Response of Annealed 2 1/4 cr – 1 Mo Steel," *Structural Materials for Service at Elevated Temperatures in Nuclear Power Generation*, MPC-1 (American Society of Mechanical Engineers, 1975).

Jennings, P. C., "Earthquake Response of a Yielding Structure," *Proceedings of ASCE, Journal of Engineering Mechanics Division*, Paper No. 4435, EM 4 (August 1965), pp 41-68.

Jhansale, H. R., "Evolution of Deformation Phenomena of Metals for Fatigue Analysis," *Journal of Testing and Evaluation, ASTM-JTEVA*, Vol 3, No. 5 (ASTM, September 1975), pp 348-354.

Jhansale, H. R., "A Friction Stress Method for the Cyclic Inelastic Behavior of Metals," *Transactions of the 3rd International Conference on Structural Mechanics in Reactor Technology*, Vol 5, L5/4 (September 1975).

Jhansale, H. R., *Inelastic Deformation and Fatigue Response of Spectrum Loaded Strain Controlled Axial and Flexural Members*, Ph.D. Dissertation (University of Waterloo, 1971).

Jhansale, H. R., "A New Parameter for the Hysteretic Stress-Strain Behavior of Metals," *Transactions of ASME, Journal of Engineering Materials and Technology*, Vol 97, Series H, No. 1 (January 1975), pp 33-38.

Jhansale, H. R. and T. H. Topper, "An Engineering Analysis of the Inelastic Stress Response of a Structural Metal Under Variable Cyclic Strains," *Cyclic Stress-Strain Behavior—Analysis, Experimentation and Failure Prediction, ASTM STP 519* (ASTM, 1973), pp 246-270.

Keshavan, S., *Some Studies on the Deformation and Fracture of Normalized Mild Steel Under Cyclic Conditions*, Ph.D. Dissertation (University of Waterloo, December 1966).

Landgraf, R. W., *Cyclic Deformation and Fatigue of Hardened Steels*, T&AM Report 320 (University of Illinois, 1968).

Landgraf, R. W., J. Morrow, and T. Endo, "Determination of the Cyclic Stress-Strain Curve," *Journal of Materials, ASTM-JMLSA*, Vol 4, No. 1 (March 1969), pp 176-188.

Mahin, S. A. and V. V. Bertero, "Nonlinear Seismic Response Evaluation—Charaima Building," *Proceedings ASCE, Journal of Structural Division* (June 1974), pp 1225-1242.

Martin, J. F., *Cyclic Mechanical Tests and an Appropriate Analytical Stress-Strain Model for A-36 Steel*, Technical Report M-86/AD780802 (U. S. Army Construction Engineering Research Laboratory, May 1974).

Martin, J. F., T. H. Topper, and G. M. Sinclair, "Computer Based Simulation of Cyclic Stress-Strain Behavior With Applications to Fatigue," *Materials, Research and Standards, MTRSA*, Vol 11, No. 2 (February 1971), pp 23-29.

Masing, G., "Eigenspannungen und Verfestingung bein Messing," *Proceedings of the 2nd International Congress of Applied Mechanics, Zurich 1926* (1926), pp 332-335.

Newmark, N. M. and E. Rosenblueth, *Fundamentals of Earthquake Engineering* (Prentice Hall, Inc. 1971).

Oldroyd, P. W. J., D. J. Burns, and P. P. Benham, "Strain Hardening and Softening of Metals Produced by Cycles of Plastic Deformation," *Proceedings Institution of Mechanical Engineers*, Vol 150 (1965-66).

Pinkham, C. W., "Procedures and Criteria for Earthquake Resistant Design—Part I," *Building Practices for Disaster Mitigation*, Building Science Series 46 (National Bureau of Standards, 1973), pp 188-208.

Popov, E. P., "Low Cycle Fatigue of Connections and Details," *Proceedings ASCE-IABSE Joint International Conference on Planning and Design of Tall Buildings*, State-of-the-Art Report No. 3, Tech. Comm. No. 18, Vol II (1972), pp 741-755.

Recommended Practice of Constant Amplitude Low Cycle Fatigue Testing, Forthcoming ASTM Standards, Part 10 (ASTM).

Rice, R. C. and R. I. Stephens, *Overload Effects on Sub-critical Crack Growth in Austenitic Manganese Steel*, ASTM STP 536 (1973), pp 95-114.

Rosenberger, P. C., *Fatigue Behavior of Smooth and Notched Specimens of Man-Ten Steel*, M. S. Thesis (T&AM Department, University of Illinois, 1968).

Segall, R. L. and J. M. Finney, "The Relation Between Physical Properties and the Observed Dislocation Distribution in Fatigued Metals," *Acta Metallurgica*, Vol II (July 1963), pp 685-690.

Seismic Design for Buildings, TM 5-809-10 (Department of the Army, 1973).

Sharma, S. K. and H. R. Jhansale, *A Plasticity Formulation for Cyclic Inelasticity Structural Analysis*, Interim Report M-202/ADA036473 (U. S. Army Construction Engineering Research Laboratory, 1977).

Smith, R. W., M. H. Hirschberg, and S. S. Manson, *Fatigue Behavior of Materials in Low and Intermediate Life Range*, NASA Technical Note D-1574 (National Aeronautics and Space Administration, April 1963).

Tuler, F. R., and J. Morrow, *Cycle Dependent Stress-Strain Behavior of Metals*, T&AM Report No. 293 (University of Illinois, March 1963).

Wetzel, R. M., *A Method of Fatigue Damage Analysis*, Technical Report No. SR 71-107 (Ford Motor Company, August 1971).

CERL DISTRIBUTION

Picatinny Arsenal
ATTN: SMUPA-VP3

US Army, Europe
ATTN: AEAEN

Director of Facilities Engineering
APO New York 09403

DARCOM STIT-EUR
APO New York 09710

West Point, NY 10996
ATTN: Dept of Mechanics
ATTN: Library

Chief of Engineers
ATTN: Tech Monitor
ATTN: DAEN-ASI-L (2)
ATTN: DAEN-FEB
ATTN: DAEN-FEZ-A
ATTN: DAEN-MCZ-S
ATTN: DAEN-RDL

ATTN: DAEN-PMS (12)
for forwarding to
National Defense Headquarters
Director General of Construction
Ottawa, Ontario K1A0K2
Canada

Canadian Forces Liaison Officer (4)
US Army Mobility Equipment
Research and Development Command
Ft Belvoir, VA 22060

Div of Bldg Research
National Research Council
Montreal Road
Ottawa, Ontario, K1A0R6

British Liaison Officer (5)
US Army Mobility Equipment
Research and Development Center
Ft Belvoir, VA 22060

Airports and Const. Services Dir.
Technical Information Reference
Centre
KA0L, Transport Canada Building
Place de Ville
Ottawa, Ontario Canada K1A0N8

US Army R&S Group (Europe)
ATTN: AMXSN-E-RM
FPO NY 09510

Ft Belvoir, VA 22060
ATTN: Learning Resources Center
ATTN: ATSE-TD-TL (2)
ATTN: Kingman Bldg, Library

US Army Foreign Science & Tech Center
ATTN: Charlottesville, VA 22901
ATTN: Far East Office

Ft Monroe, VA 23651
ATIN: ATEN
ATTN: ATEN-FE-BG (2)

Ft McPherson, GA 30330
ATTN: AFEN-FED

USA-WES
ATTN: Concrete Laboratory
ATTN: Library

USA-CRREL

6th US Army
ATTN: AFKC-LG-E
I Corps (ROK/US) Group
I Corps (ROK/US) Group
ATTN: EACI-EN

US Army Engineer District
Saudi Arabia
ATTN: Library
New York
ATTN: Chief, Design Br
Buffalo
ATTN: Library
Pittsburgh
ATTN: Library
ATTN: Chief, Engr Div
Philadelphia
ATTN: Library
ATTN: Chief, NAPEN-D

US Army Engineer District
Baltimore
ATTN: Library
ATTN: Chief, Engr Div
Norfolk
ATTN: Library
ATTN: Chief, NAOEN-D
Huntington
ATTN: Library
ATTN: Chief, ORHED-D
Wilmington
ATTN: Chief, SAWEN-DS
Charleston
ATTN: Chief, Engr Div
Savannah
ATTN: Library
ATTN: Chief, SASAS-L
Jacksonville
ATTN: Library
ATTN: Const. Div
ATTN: Design Br, Structures Sec.
Mobile
ATTN: Library
ATTN: Chief, SAMEN-D
Nashville
ATTN: ORNED-D
Memphis
ATTN: Chief, LMMED-DT
Vicksburg
ATTN: Chief, Engr Div
Louisville
ATTN: Chief, Engr Div
Detroit
ATTN: Library
ATTN: Chief, NCEED-T
St. Paul
ATTN: Chief, ED-D
Chicago
ATTN: Chief, NCCED-DS
Rock Island
ATTN: Chief, NCRED-D
ATTN: Chief, Engr Div
St. Louis
ATTN: Library
ATTN: Chief, ED-D
Kansas City
ATTN: Library (2)
ATTN: Chief, Engr Div
Omaha
ATTN: Chief, Engr Div
New Orleans
ATTN: Library (2)
ATTN: Chief, LMNED-DG
Little Rock
ATTN: Chief, Engr Div
Tulsa
ATTN: Chief, Engr Div
ATTN: Library
Fort Worth
ATTN: Library
ATTN: Chief, SWFED-D
Galveston
ATTN: Chief, SWGAS-L
ATTN: Chief, SWGED-DS
Albuquerque
ATTN: Library
ATTN: Chief, Engr Div
Los Angeles
ATTN: Library
ATTN: Chief, SPLED-D
San Francisco
ATTN: Chief, Engr Div
Sacramento
ATTN: Chief, SPKED-D
Far East
ATTN: Chief, Engr
Japan
ATTN: Library
Portland
ATTN: Library
ATTN: Chief, DB-6
Seattle
ATTN: Chief, NPSCO
ATTN: Chief, EN-DB-ST
Walla Walla
ATTN: Library
ATTN: Chief, Engr Div
Alaska
ATTN: Library
ATTN: Chief, NPADE-R

US Army Engineer Divistion
Europe
ATTN: Technical Library
New England
ATTN: Library
ATTN: Chief, NEDED-T

US Army Engineer Division
North Atlantic
ATTN: Library
ATTN: Chief, NADEN-T
Middle East (Rear)
ATTN: MEDED-T
South Atlantic
ATTN: Chief, SADEN-TS
ATTN: Library
Huntsville
ATTN: Library (2)
ATTN: Chief, HNDED-CS
ATTN: Chief, HNDED-SR
Lower Mississippi Valley
ATTN: Library
Ohio River
ATTN: Library
ATTN: Chief, Engr Div
North Central
ATTN: Library
ATTN: Chief, Engr Div
Missouri River
ATTN: Library (2)
ATTN: Chief, MRDED-T
Southwestern
ATTN: Library
ATTN: Chief, SWDED-TS
South Pacific
ATTN: Chief, SPDED-TG
Pacific Ocean
ATTN: Chief, Engr
ATTN: FM&S Branch
ATTN: Chief, PODED-D
North Pacific
ATTN: Chief, Engr Div

Facilities Engineers
Ft Campbell, KY 42223
Ft Hood, TX 76544
FORSCOM
Ft Devens, MA 01433
Ft Lewis, WA 98433 (2)
Ft Carson, CO 80913
TRADOC
Ft Dix, NJ 08640
Ft Monroe, VA 23651
Ft Gordon, GA 30905
Ft Knox, KY 40121
Ft Sill, OK 73503
Ft Bliss, TX 79916
DSCPER
West Point, NY 10996
USAIC (2)
Ft Benning, GA 31905
USAAVNC
Ft Rucker, AL 36361
CAC&FL (2)
Ft Leavenworth, KS 66027
AMC
Duqway, UT 84022
USACC
Ft Huachuca, AZ 85613
HQ, 1st Inf Div & Ft Riley, KS 66442
HQ, 5th Inf Div & Ft Polk, LA 71459
HQ, 7th Inf Div & Ft Ord, CA 93941
HQ, 24th Inf & Ft Stewart, GA 31313

AF Civil Engr Center/XRL
Tyndall AFB, FL 32401

Little Rock AFB
ATTN: 314/DEEE (Mr. Gillham)

AFWL/DES
Kirtland AFB, NM 87117

Naval Air Systems Command
WASH DC 20360

NAVFAC/Code 04
Alexandria, VA 22332

Port Hueneme, CA 93043
ATTN: Library (Code L08A)

Washington, DC
ATTN: Building Research Advisory Board
ATTN: Transportation Research Board
ATTN: Library of Congress (2)
ATTN: Dept of Transportation Library

Defense Documentation Center (12)

Engineering Societies Library
New York, NY 10017

R. T. Shield
212 Talbot Lab
University of Illinois
Urbana, IL 61801

JoDean Morrow
321 Talbot Lab
University of Illinois
Urbana, IL 61801

H. T. Corten
321 Talbot Lab
University of Illinois
Urbana, IL 61801

T. H. Topper
Dept of Civil Engineering
University of Waterloo
Waterloo, Ontario
Canada

R. W. Swindeman
Metals and Ceramics
Oak Ridge National Lab
PO Box X
Oak Ridge, TN 37830

D. R. Diericks
Materials Science Division
Argonne National Lab
9700 S. Cass Ave
Argonne, IL 60439

L. F. Coffin Jr.
Metallurgy and Ceramics Lab
General Electric Company
Research and Development Center
PO Box 8
Schenectady, NY 12301

Erhard Krempl
Dept of Mechanical Engineering
Rensselaer Polytechnic Institute
Troy, NY 12181

Carle Jaske
Structural Mechanics Section
Battelle Columbus Lab
505 King Ave
Columbus, OH 43201